

Stability of Quantum Dot Solar Cells: A Matter of (Life)Time

Miguel Albaladejo-Siguan, Elizabeth C. Baird, David Becker-Koch, Yanxiu Li, Andrey L. Rogach, and Yana Vaynzof*

Colloidal quantum dot solar cells (QDSCs) are promising candidates amongst third generation photovoltaics due to their bandgap tunability, facile low-temperature ink processing, strong visible-to-infrared absorption, and potential for multiple-exciton generation. An unprecedented increase in power conversion efficiency is reported for different types of QDSCs in the last few years, making them appealing for large-scale fabrication. The stability of QDSCs, however, still remains inadequate for industrial application, especially when they are operated under a sun-like illumination in an ambient atmosphere. This review focuses on three classes of QDs (lead chalcogenides, lead halide perovskites, and lead-free QDs) and considers the current understanding of their degradation mechanisms. For each material class, strategies for stability improvement are discussed, both from materials science and device engineering perspectives. This paper concludes by suggesting a methodology for characterizing the QDSCs' stability which would standardize the results obtained by researchers worldwide.

others. QDs can be made from a single atomic species, like silicon, or compound semiconductors, such as Cd or Pb chalcogenides.^[1,2] In the field of photovoltaics, the most widely studied QDs are lead chalcogenides (PbX, with X = S, Se, Te), or most recently metal halide perovskite QDs. QDs are also widely used in luminescence-related applications, such as in light-emitting diodes (LEDs) and fluorescent biomarkers. In these applications, so-called core-shell QDs are often utilized, where cadmium chalcogenides with wide-bandgap semiconductor shells are just one example.^[3–5] QDs have also found their way into a few other technologies—InAs QDs have been used in solid-state lasers,^[6] while PbS QDs—as CO₂ catalysts.^[7] The unique surface properties of QDs have even made their own field of study. Due to their small size, high percentage of atoms in a QD are

situated at the surface—≈25% for a 2 nm QD, just to make an example.^[8] The QD surface is commonly covered by passivating molecules called ligands, which may belong to various classes—organic or inorganic, monodentate or bidentate, monoatomic or long-chained; these ligands can be used to functionalize QDs on demand, depending on their desired usage (Figure 1). No matter what their final application is, QDs must have one characteristic in common: the long-term stability, because all of the aforementioned applications rely on stable QDs whose lifetimes should surpass years in the best-case scenario. The motivation for such a long-term stability may be economic in nature, as it is the case of commercial-scale solar cells or light-emitting diodes (LEDs). For biological applications, stability is even more important, since degradation could mean generation of toxic by-products dangerous to the living organisms.


In this review, we will focus on the stability of colloidal quantum dot solar cells (QDSCs). This emerging photovoltaic technology has been researched for more than a decade and rapidly reached high power conversion efficiencies (PCEs), such as the 14% for a PbS or 16.6 % for a perovskite QDSC as reported recently by Kim et al.^[9] and by Hao et al.,^[10] respectively. Unfortunately, even though the PCEs of QDSCs have been steadily increasing, the device stability remains at the lower end when compared to industrial standards. In many publications, the lifetime of the fabricated solar cells is tested in environments which avoid stress factors that are normally present in normal application. On top of that, many publications use a slightly different method to determine the stability of the cells, which complicates a direct comparison between different studies. Many advances have been made toward more

1. Introduction

Nanocrystals of semiconducting materials have attracted the interest of investigators ever since their remarkable potential for optoelectronic applications was discovered. Once the size of nanocrystals is smaller than their corresponding Bohr exciton radius these materials are named quantum dots, due to the quantum confinement effect that determines their physical properties. These colloidal quantum dots (QDs), offer several useful characteristics: a size-tunable bandgap, narrow emission spectra, and ambient-air solution processability, among

M. Albaladejo-Siguan, E. C. Baird, D. Becker-Koch, Dr. Y. Li, Prof. Y. Vaynzof
Integrated Center for Applied Physics and Photonic Materials (IAPP)
and Center for Advancing Electronics Dresden (cfaed)
Technische Universität Dresden
Nöthnitzer Straße 61, Dresden 01187, Germany
E-mail: yana.vaynzof@tu-dresden.de

Dr. Y. Li, Prof. A. L. Rogach
Department of Materials Science and Engineering, and Centre
for Functional Photonics (CFP)
City University of Hong Kong
83 Tat Chee Avenue, Kowloon, Hong Kong SAR, P. R. China

 The ORCID identification number(s) for the author(s) of this article can be found under <https://doi.org/10.1002/aenm.202003457>.

© 2021 The Authors. Advanced Energy Materials published by Wiley-VCH GmbH. This is an open access article under the terms of the Creative Commons Attribution License, which permits use, distribution and reproduction in any medium, provided the original work is properly cited.

DOI: 10.1002/aenm.202003457

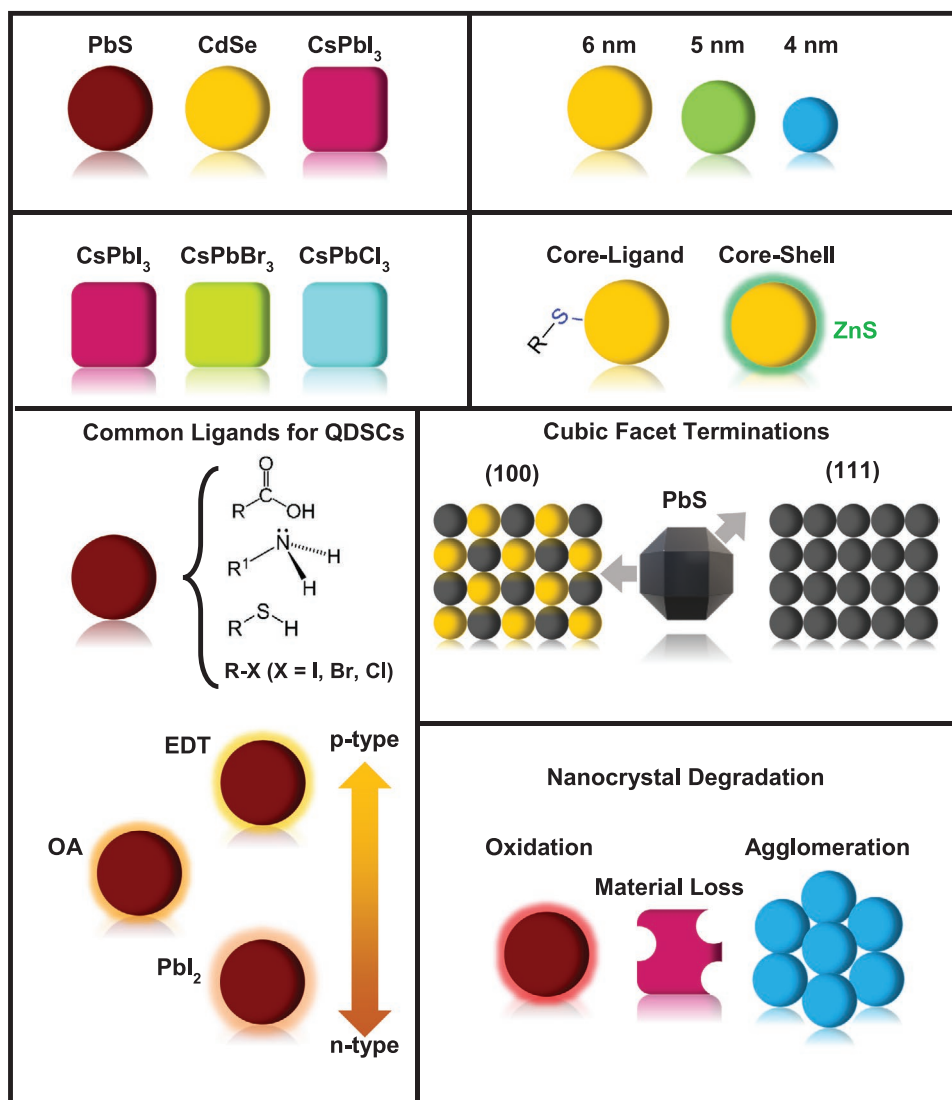


Figure 1. Sketch summary of several QD materials found in solar cell applications. Their optoelectronic characteristics are tuned by the core size/ composition and the surface ligand passivation. In the bottom left panel, EDT and OA stand for 1,2-ethanedithiol and oleic acid ligands, which are very common in solar cell applications. In the last panel, three typical pathways of QD degradation are shown.

stable QDSCs in the past years, and these will be discussed in the following sections both from materials science and device engineering perspectives. Several principal QD materials will be covered separately: lead chalcogenide QDs, lead halide perovskite QDs, and lead-free QDs.

2. Lead Chalcogenide Quantum Dots

Lead chalcogenides are versatile semiconducting materials that have been used in optoelectronic devices since before the Second World War,^[11] and were more recently used as a component in third-generation solar cells. QDs made from lead sulfide, selenide, and telluride (PbX: PbS, PbSe, and PbTe) have properties that make them particularly useful as photovoltaic light harvesters. Due to their large Bohr radii and strong quantum confinement effects,^[12] PbX QDs have extensive interdot wavefunction

overlap,^[13] leading to superior electronic coupling. Their solution-based syntheses are relatively low-cost and scalable, and can be modified to produce QDs with a range of desired bandgaps. While this class of materials holds high potential for photovoltaic applications, their tendency to degrade in ambient conditions presents a significant challenge. In this chapter, we will discuss the causes of degradation of PbX QDs, both in the active QD layer and in other constituent layers. Then, some common strategies for improving stability of PbX will be presented.

2.1. Background and Material Properties

Of the three lead chalcogenides, lead sulfide (PbS) has been so far the most studied and successfully utilized in photovoltaic applications. Like PbSe and PbTe, it has a rock-salt cubic crystal structure. The bulk bandgap of PbS is 0.4 eV, which

can be increased up to 2.3 eV by reducing the QD diameter to 1.8 nm.^[14] PbS bulk crystals were employed since the 1950s as the most common sensor material for infrared detectors.^[15] The use of this material for QDSCs dates back to the early 2000s, with the pioneering work by McDonald et al.^[16] who incorporated them in solution-processed photovoltaics. Since then, the performance of PbS QDSCs has steadily increased to the most recent record PCE of 14% in 2020.^[9,17,18] The most common way to synthesize PbS QDs is the so-called “hot-injection synthesis,”^[19] which involves the injection of bis(trimethylsilyl) sulfide into a solution of lead oxide (PbO) and oleic acid, resulting in lead sulfide nanocrystals covered by oleate ligands.

Lead selenide and telluride are two other good options for QDSC materials. In fact, some of their properties make them potentially superior to PbS in the context of photovoltaic application. For example, their larger exciton Bohr radii as compared to PbS (18 nm for PbS,^[20] 46 nm for PbSe,^[21] and 150 nm for PbTe^[22]) lead to an increased electronic coupling and offer the possibility for multiple electron generation (MEG).^[23] External quantum efficiencies of over 100% via MEG have already been demonstrated in lead telluride solar cells.^[24] While PbSe and PbTe hold promise, their use in photovoltaics has been hindered by

their much lower resistance to oxidative degradation as compared to PbS.^[25] This higher susceptibility to oxidation stems from the reduced electronegativity of selenium and tellurium as compared to sulfur.^[26–28] Utilizing these chalcogenides in photovoltaic applications therefore requires a more extensive approach in terms of surface engineering, as will be discussed in upcoming sections.

2.2. Degradation Factors

2.2.1. Active Layer Degradation

There are a number of reasons that contribute to the loss of performance in QDSCs, but the main cause of ambient degradation of PbX QDs is surface oxidation.^[25,27–30] Additional factors like ultraviolet and visible light exposure can accelerate the process of surface oxidation,^[14,25] but have little effect on PbX QDs in an air-free environment.^[31,32] Oxidation affects the electronic properties of PbX QDs primarily by shrinking the effective core size, while creating a shell of oxidative products on the surface (Figure 2a). The chemical composition of these surface products can include PbO and Pb(OH)₂, with additional

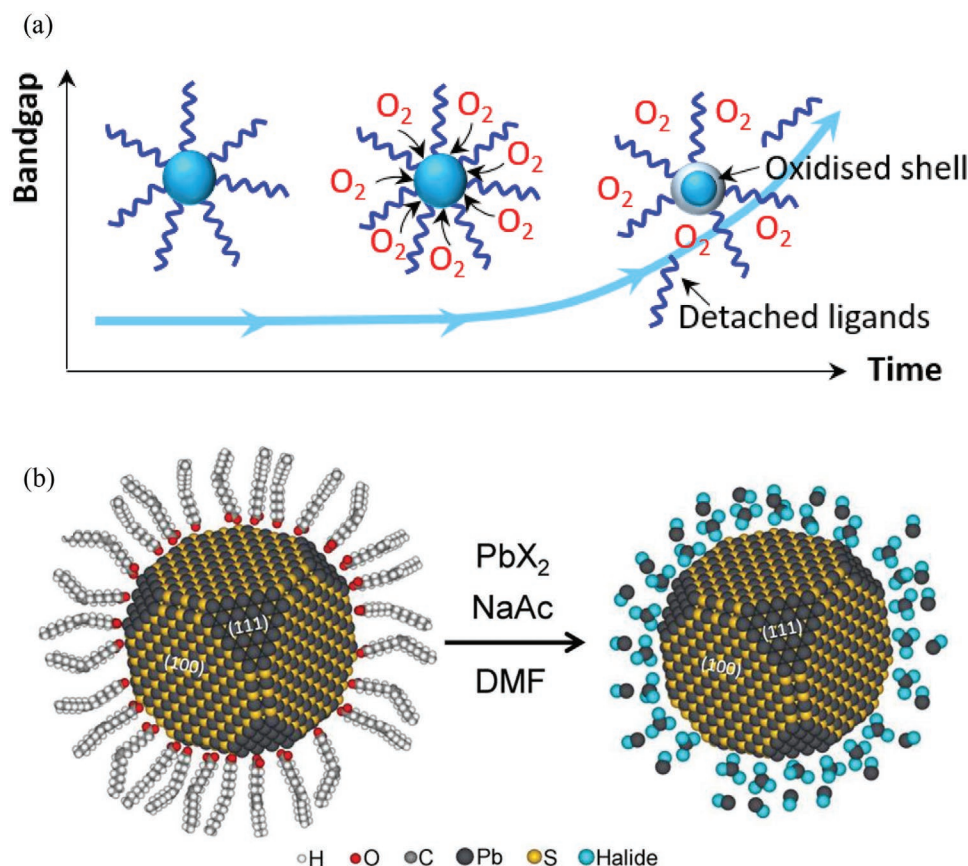


Figure 2. a) Evolution of the composition of a PbSe QD as it undergoes oxidation. Oxygen molecules bind to the surface, and within hours an oxide shell is formed, reducing the effective size of the core (and thus increasing the bandgap), and leading to partial detachment of ligands. Reproduced with permission.^[32] Copyright 2010, American Chemical Society. b) Illustration of structural changes of a PbS QD in the process of ligand exchange with lead halides (PbX₂) and sodium acetate (NaAc) using dimethylformamide (DMF) as solvent. The [111] facets consist of a single element, while the [100] facets have an alternating pattern of Pb and S. Ligands bind preferentially to the [111] facet, making this site more resistant to oxidation. Reproduced with permission.^[39] Copyright 2019, John Wiley and Sons.

SeO₂, and SeO₃[−] in lead selenide,^[33] and PbSO₃ with PbSO₄ in lead sulfide.^[34,35] Surface oxidation has a contrasting effect on device performance depending on the duration of exposure to the ambient. In PbS-based QDSCs, it has been found that the thin layer of PbO created upon initial air exposure helps in slowing down the initial degradation or even shortly improving device performance.^[35,32] This thin PbO shell blocks pathways for bimolecular recombination and leakage currents, while influencing the QD energy levels.^[35,36,37] Conversely, this initial oxidation-assisted performance improvement has not been observed in PbSe devices. Since PbSe is much more sensitive to oxygen than PbS, this observation is not too surprising—it is likely that PbSe oxidation occurs too rapidly for any initial enhancement to be measurable. It has been shown that the short-term oxidative emission quenching in PbSe QDs can be reversed by placing them in an O₂-free environment.^[32] In the long-term, exposure of both lead sulfide and selenide to ambient air will produce similarly detrimental effects. Oxidative PbSO₃, PbSO₄, SeO₂, and SeO₃[−] generate trap states.^[27] The formation of these oxides will eventually lead to irreversible changes in their optoelectronic and electrical properties.^[38] These changes are evidenced by a blue-shift in absorption spectra associated with an effective core shrinkage. The thickening of the oxide shell will first reduce the electronic coupling, and then prevent charge transfer altogether.^[37] These effects will deteriorate the semiconducting nature of the QD layer, turning it largely into an insulator, and thus leading to a significant decline in performance of a solar cell.

While oxidation is the main cause of ambient degradation of PbX QDs, there are several factors that can influence this process. Humidity can affect the stability through the binding of water molecules onto the QD surface and upon a long-term exposure can be detrimental to the solar cell performance. H₂O does not react with surface constituents to create new products, but it can bind to the QDs' surface via OH[−] groups. This binding can have a protective effect, particularly during device fabrication. The OH[−] groups can sterically block O₂ molecules and temporarily slow down the oxidation.^[35,40,41] Light exposure is another ambient effect, which is known to accelerate the loss of performance over time in PbX QDSCs. Interestingly, it has been found that light-induced degradation of solar cells can be reversed by storing them in the dark.^[42] In colloidal PbSe QDs, UV irradiation can speed up the oxidation-induced blue shift of the first excitonic peak when the measurement is made in ambient air.^[32] No UV-induced blue-shift was observed when the same experiment was performed in a N₂ atmosphere, which implies that UV exposure does not cause degradation of PbSe QDs on its own, but rather accelerates the process of oxygen-induced degradation.^[32]

The severity of oxidative effects in lead chalcogenide QDs is largely influenced by their surface properties, which are related to their crystal structure.^[43] PbX has a rock-salt cubic structure, where the [100] and [111] facets are especially of relevance.^[44–46] The ratio of [100] facets to [111] facets on the QD surface plays a large role in the overall stability of the material, as these possess contrasting properties. PbX [100] sites are made up of a stoichiometric ratio of both Pb atoms and S, Se or Te atoms, arranged in a checkerboard-type pattern (Figure 2b). These [100] sites are fully coordinated and charge neutral. The [111]

faces, on the other hand, consist entirely of a single element, i.e., either Pb or S/Se/Te. These PbX [111] facets are undercoordinated and possess dangling bonds, where ligands will bind preferentially. Surface quantification studies have shown that PbX QDs have an excess of lead atoms,^[47,48] which is significant in terms of ligand binding. It was shown that the number of ligands in oleate-capped PbX QDs correlates directly with the amount of excess surface Pb, with one ligand for each excess surface lead atom according to Moreels et al.,^[49] or one oleate ligand for every two surface Pb, according to Katsiev et al.^[50]

The size of PbX QDs also influences their degradation dynamics.^[51–55] The smallest PbX nanoparticles often have an octahedral shape, which has a high ratio of [111] to [100] facets. As the dots grow larger, their shape evolves first into a truncated octahedron, then eventually into a cuboctahedron, and the ratio of facets skews in favor of the [100] type (Figure 3). As ligands bind preferentially to the [111] faces of PbX QDs, a higher ratio of [100] sites leads to a less-dense ligand coating and a lowered oxidation resistance.^[31,56,57]

Surface properties of PbX QDs may easily change even prior to their integration into solar cells. When stored in solution after the synthesis, the QDs have been shown to undergo a narrowing of the size distribution.^[58] This narrowing is driven in part by the different surface energies of the open-lying facets of PbX nanocrystals.^[43,44] Early in the synthesis, small cluster-like particles are formed, which may later separate from the crystals they were attached to as they are dispersed and stored in a solvent. The reason for this detachment can be either a mismatch between the crystal facets or a shape change of the crystals to the more energetically favorable [111] faces by shedding of small clusters. Another process that may occur when the QDs are dispersed in solution as a colloidal ink is the agglomeration of dots and their subsequent precipitation. Thus, the choice of organic ligands with a suitable length can greatly influence the steric hindrance between the dots and determine the colloidal stability of the ink. For example, the addition of a longer-chained hexylamine to a butylamine-only ink medium has been shown to enhance its stability.^[59]

2.2.2. Degradation of Charge Extraction Layers in Solar Cells

While the previous section focused solely on the stability of the device active layer, one must consider that a photovoltaic diode is a stack of several functional layers. The extraction layers—electron-transport layer (ETL) and hole transport layer (HTL) that sandwich the PbX active layer are not immune to the effects of degradation, and play an important role in determining the lifetime of the device.^[60] To illustrate this, we will consider some common extraction layers used in PbX solar cells.

The ETL resides between the ITO electrode and the PbX QD film. The ETL can be made from the oxides of tin,^[61] titanium,^[62] or zinc,^[63] where zinc oxide (ZnO) is the most common one to be used. While ZnO is far more air-stable than the PbX QDs, it may also be influenced by environmental factors. The synchronization between the ETL and the PbX layers must be fine-tuned, in terms of film smoothness, work functions, and charge carrier recombination.^[62,63] Any of these factors can affect the stability of solar cells, as was shown in

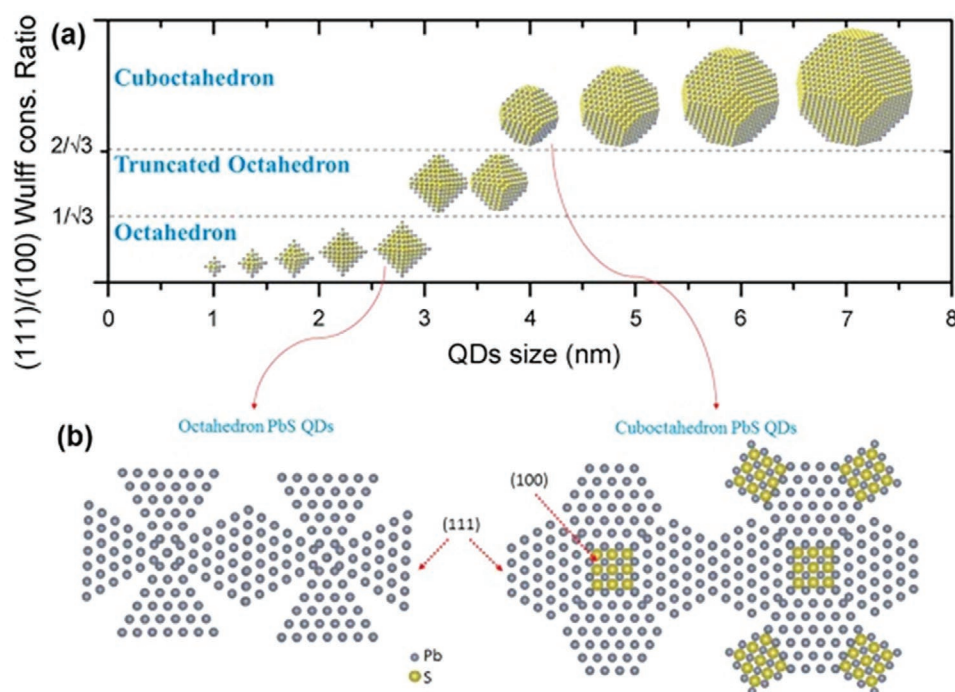


Figure 3. The relationship between PbS QD size, morphology and facet ratio: a) the shape of the dots depending on their size. Smaller dots, pictured here as 3 nm and under, have an octahedral shape and a high ratio of surface [111] facets. Larger dots, roughly 4 nm and above, have a cuboctahedral structure and a larger ratio of [100] facets. b) the surface for the two different shapes of QDs. Reproduced with permission.^[55] Copyright 2018, Elsevier.

Kirman's study of ZnO ETLs modified with In_2O_3 .^[64] It was found that exposure of ZnO layers to UV irradiation shifts the material's work function and increases carrier recombination, causing a loss of PCE over months. Adding an In_2O_3 layer ameliorated some of these effects, resulting in a remarkable maintenance in efficiency over time as compared to bare ZnO. The In_2O_3 -treated device maintained 100% of its PCE after 5 months in air, while the control device maintained only 80%. After 5 h under continuous UV irradiation, the In_2O_3 -treated device sustained 80% of its initial PCE while the control device only 60%.

Another important factor in stabilizing PbX QDSCs is the interplay between the active layer and the HTL, which can be illustrated by using MoO_3 . When MoO_3 is exposed to oxygen, its work function can shift, and in a device containing both MoO_3 and PbS QDs, oxidation of MoO_3 can in turn cause PbS to degrade. Specifically, a Schottky barrier is formed when the Fermi level pinning of the MoO_3 is disturbed by oxygen, thereby affecting device stability without a direct material decomposition.^[65] This phenomenon was confirmed by the introduction of the now-ubiquitous 1,2-ethanedithiol (EDT) as a ligand for EDT-PbS hole extraction layers.^[34,66,67] It was found that omitting MoO_3 from the solar cells not only improved their performance, but also their stability. Since then, the use of EDT-PbS layer as an HTL has become an important component in many record-setting solar cell devices.^[68–71] Apart from introducing the EDT, Chuang et al.^[2] laid the focus on another peculiarity of a PbS QD cell, namely that its performance first improves after oxygen exposure and only then starts to decline. This may only in part be attributed to the aforementioned surface oxidation, which initially reduces leakage and recombination. The improvement in performance also stems from an energy level

interplay between the active layer and the EDT-PbS layer.^[35] It has been shown that the respective energy levels shift under oxidation, which happens at unequal rates due to the different ligands used in each layer.^[29,35,72] Additionally, the bandgap of the QD film increases with progressing oxidation, due to the quantum confinement effect. This creates an interesting sequence of events in the energetic landscape of the solar cells. First, electron blocking through the EDT is improved via an increase in barrier height. This is followed by PbS QD decomposition within the EDT layer, resulting in a decrease in charge transport and the ultimate demise of the device (Figure 4).^[35]

The use of EDT in solar cells has not changed much in the last years, mainly due to the unique properties of this molecule. EDT possesses two SH- groups, so it can fold itself to bind twice to the surface of the QD.^[41] If both -SH groups bind to the QD, desorption of hydroxyl ions will occur, leading to an improved QD surface. This dual thiol binding is unfortunately difficult to control in practice, which is apparent in the wide variation in performance between devices employing the same structures. Efforts to replace the EDT layer have been made through choosing different ligands or introducing an additional layer.^[73–76] For example, inserting an ultrathin NiO layer between the EDT and the gold electrodes strongly enhances the stability of the solar cells, which maintain 95% of their initial performance after heating to 80 °C for 2 h.^[77] Alternatively, one can reduce the number of access sites for oxygen absorption by using a different size of PbS QDs in the EDT layer versus the PbX active layer.^[78] A particularly promising route to replace EDT was recently suggested by Biondi et al., who used malonic acid instead of EDT, leading to an increase in the photovoltaic performance and device stability.^[79] Another approach is based

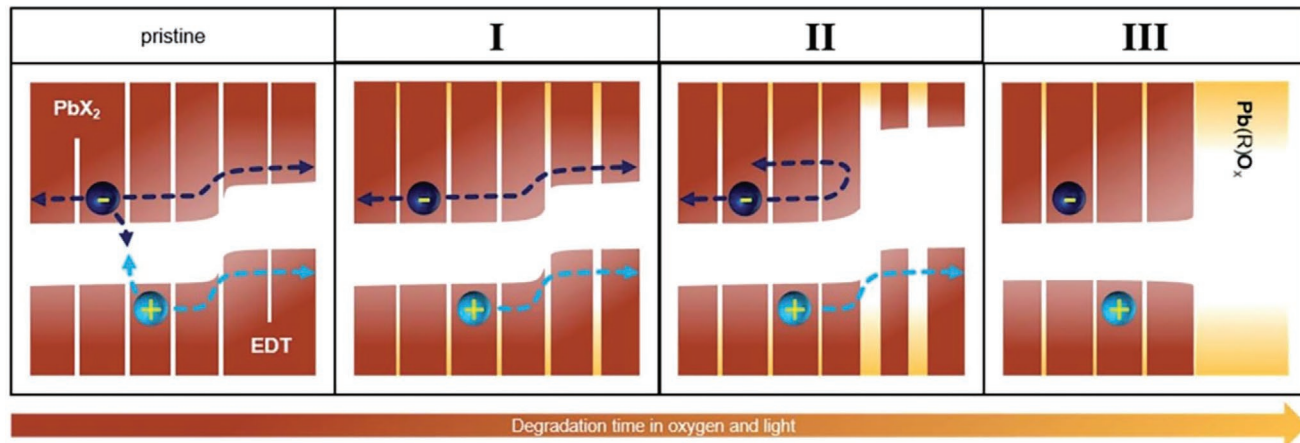
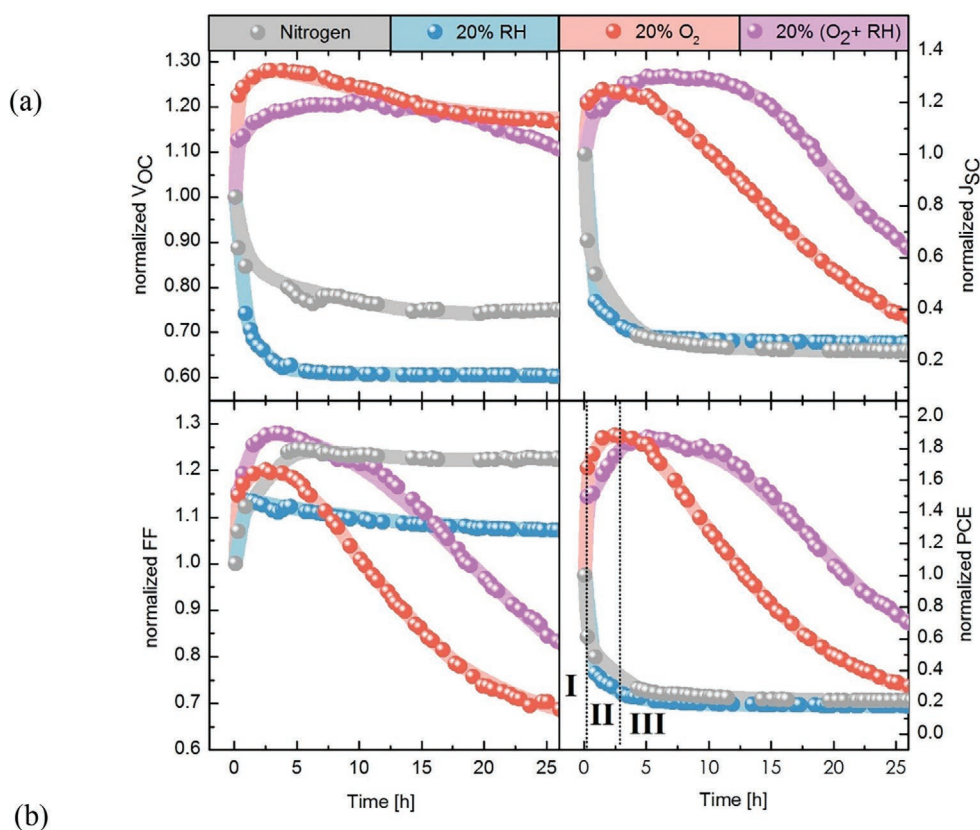


Figure 4. a) Degradation of PbS QDSCs in different environments under constant one-sun illumination. b) Changes in the energy landscape of a PbS QDSC with an EDT extraction layer during operation in an oxygenated environment. In the pristine state (before oxygen exposure) surface traps are present, so charge recombination between dots is uninhibited and leakage pathways remain open. Phase I occurs upon initial exposure to oxygen and light and lasts for several minutes. Oxidation of the surface creates a beneficial thin shell around the dots, preventing bimolecular recombination. During this phase, the performance of the cell increases. In Phase II, the EDT-covered dots degrade quickly, which increases the bandgap of the electron blocking barrier between the active and the extraction layer, enabling efficient blocking. The performance increases again in this phase, which lasts for a few hours. Phase III brings the degradation of the device, and occurs after a period of hours in air. Degradation of the extraction layers continues until the material itself decomposes. This negates any photovoltaic electronic properties and the device stops working. Reproduced with permission.^[35] Copyright 2019, Royal Society of Chemistry.

on the replacement of the EDT-QD layer by an organic HTL, such as polythieno[3,4-*b*]-thiophene-*co*-benzodithiophene (PTB7) or triisopropylsilyl ethynyl (TIPS) derivatized benzo[1,2-*b*:4,5-*b'*]-dithiophene (BDT).^[80,81] While this approach showed promising results, the stability of the transport layers needs to be improved further.^[82–88]

Another interesting passivation route involves the introduction of a layer of carbon nanotubes between the EDT layer and the gold anode, as reported by Salazar-Rios et al.^[74] in 2018. It was found that a single-walled carbon nanotube (SWCNT) layer significantly improved cell stability under illumination, which maintained 85% of its initial PCE after 105 h of continuous

light soaking in ambient air. This was in sharp contrast with the control device, which retained only 25% of its initial efficiency (Figure 5). Similar tests performed in a N_2 environment showed no additional benefits for the stability of the SWCNT-modified cells, which suggests that this layer served as an efficient barrier against oxidation. In general, the choice of stable extraction and electrode layers is one of the main methods to improve the stability of the overall device. For QDSCs, an improved passivation of the QD surface is another way to enhance their stability, which will be covered in the next section.^[89]

2.3. Strategies for PbX QDSC Stability Enhancement

A common approach to enhance the oxidation resistance of PbX QDs is their surface passivation via halides. This approach relies on the binding of halide ions to the Pb atoms on the surface, thereby reducing the number of sites where O_2 can adsorb (Figure 6). Halide passivation can be performed either in situ or postsynthesis, that is, either during the QD synthesis or afterward. One popular route of in situ passivation for solar cells is via cation exchange between CdSe and $PbCl_2$.^[26,90–92] Instead of synthesizing PbSe QD directly, CdSe QDs are treated with $PbCl_2$, leading to an exchange of cadmium cations to lead cations. This results in PbSe QDs with chloride-passivated Pb sites, and has the added benefit of passivation of the Se sites

by cadmium. This method has also been used by Kim et al.^[93] using ZnSe instead of CdSe. ZnSe has the ability to exchange cations both with PbI_2 and $PbBr_2$ in addition to $PbCl_2$, while CdSe is limited to $PbCl_2$. This offers a greater flexibility in choice of materials, since iodide and bromide can be used in addition to chloride. Nonetheless, the ZnSe route is not used as often as CdSe one, possibly because Zn does not seem to have the same passivation-enhancing properties as cadmium.^[94] A more direct approach to cadmium chloride passivation is based on the injection of a solution of $CdCl_2$ into the reaction solution just after the QD growth period is completed. This approach was demonstrated for both PbSe and PbTe solar cells.^[25,54]

Halide treatments may also be implemented after QD synthesis, either in a solution-phase or through the solid-state ligand exchange. One of the earliest successful attempts to utilize halide passivation was reported by Bae et al.^[95] in 2012, where it was demonstrated that PbSe QDs treated with molecular chlorine were more air-stable than those without treatment. Further studies revealed that other halides could also be used for PbSe QD passivation. A noteworthy example for this was reported by Zhang et al.^[96] in 2015. The authors performed a comparison between oleate-capped PbSe QD films passivated with tetrabutylammonium salts of Cl, Br, I, or F. Absorption spectra (Figure 7) have shown that the tetrabutylammonium fluoride treated film deteriorated within several hours, which is in agreement with other unsuccessful attempts to use fluoride

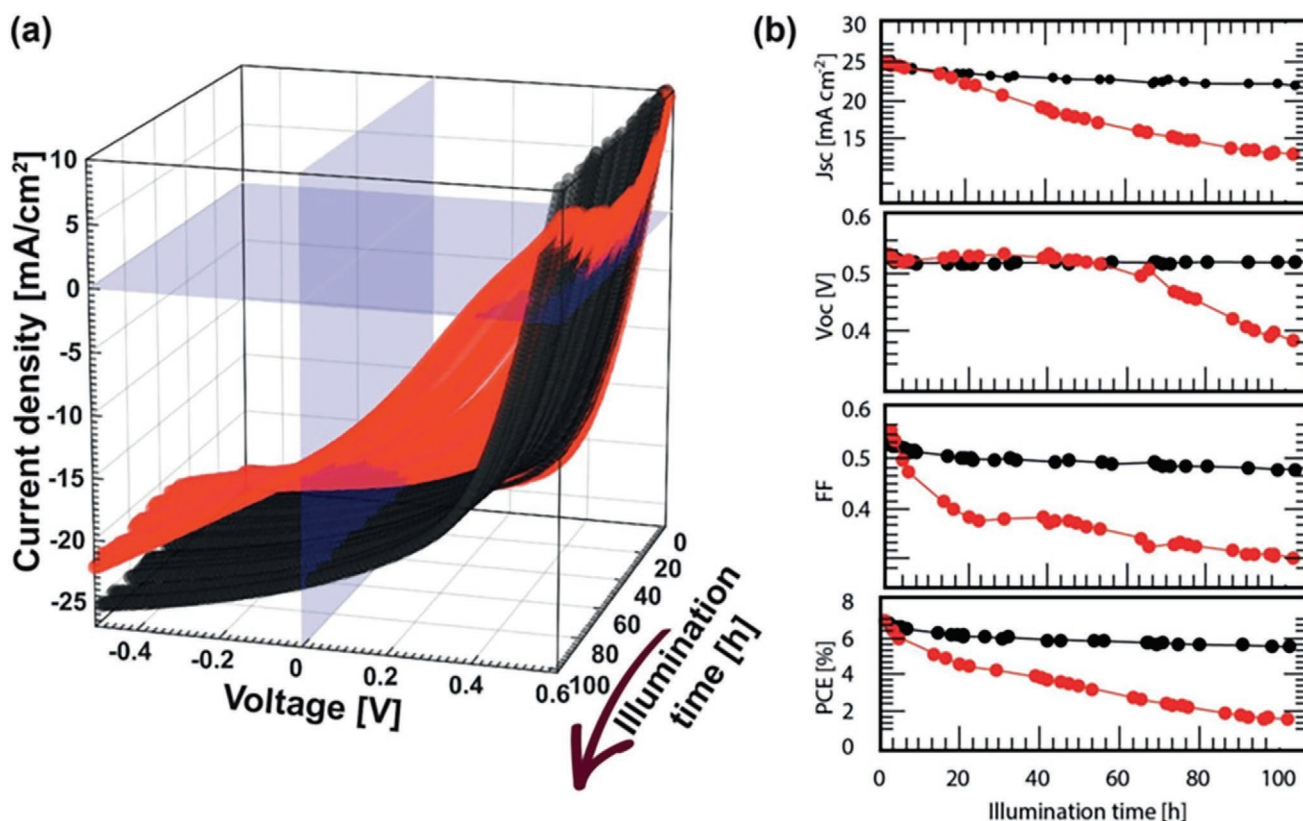


Figure 5. Performance evolution of a PbS QD-EDT device under constant solar illumination for 105 h. a) IV -curves of a device modified by a thin layer of SWCNT between the EDT layer and the gold anode (black) versus a control device (red). b) The corresponding PV parameters plotted over time. The SWCNT layer blocks the accessibility of the QDs layers by oxygen, thereby prolonging the device lifetime. Reproduced with permission.^[74] Copyright 2018, John Wiley and Sons.

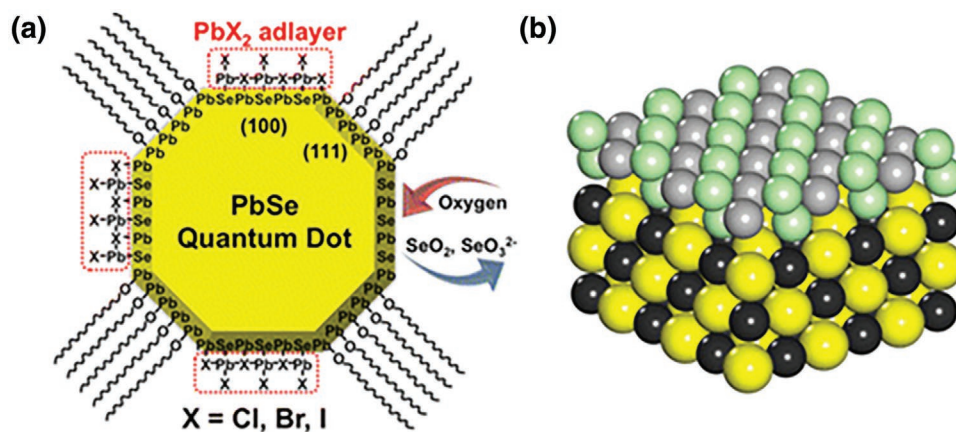


Figure 6. Illustration of the effects of oxidation and passivation on a PbSe QD. a) All Pb [111] facets are shown fully covered by oleate ligands, which protects the PbSe [111] from oxygen via steric hindrance. Three of the four [100] facets are passivated by lead halides, with Pb atoms blocking the Se [100] sites, and halide atoms blocking the Pb [100] sites. b) The right-hand [100] facet is shown unpassivated. Oxygen reacts with selenide to produce an undesirable oxide layer, depicted in gray and mint green. Reproduced with permission.^[53] Copyright 2014, American Chemical Society.

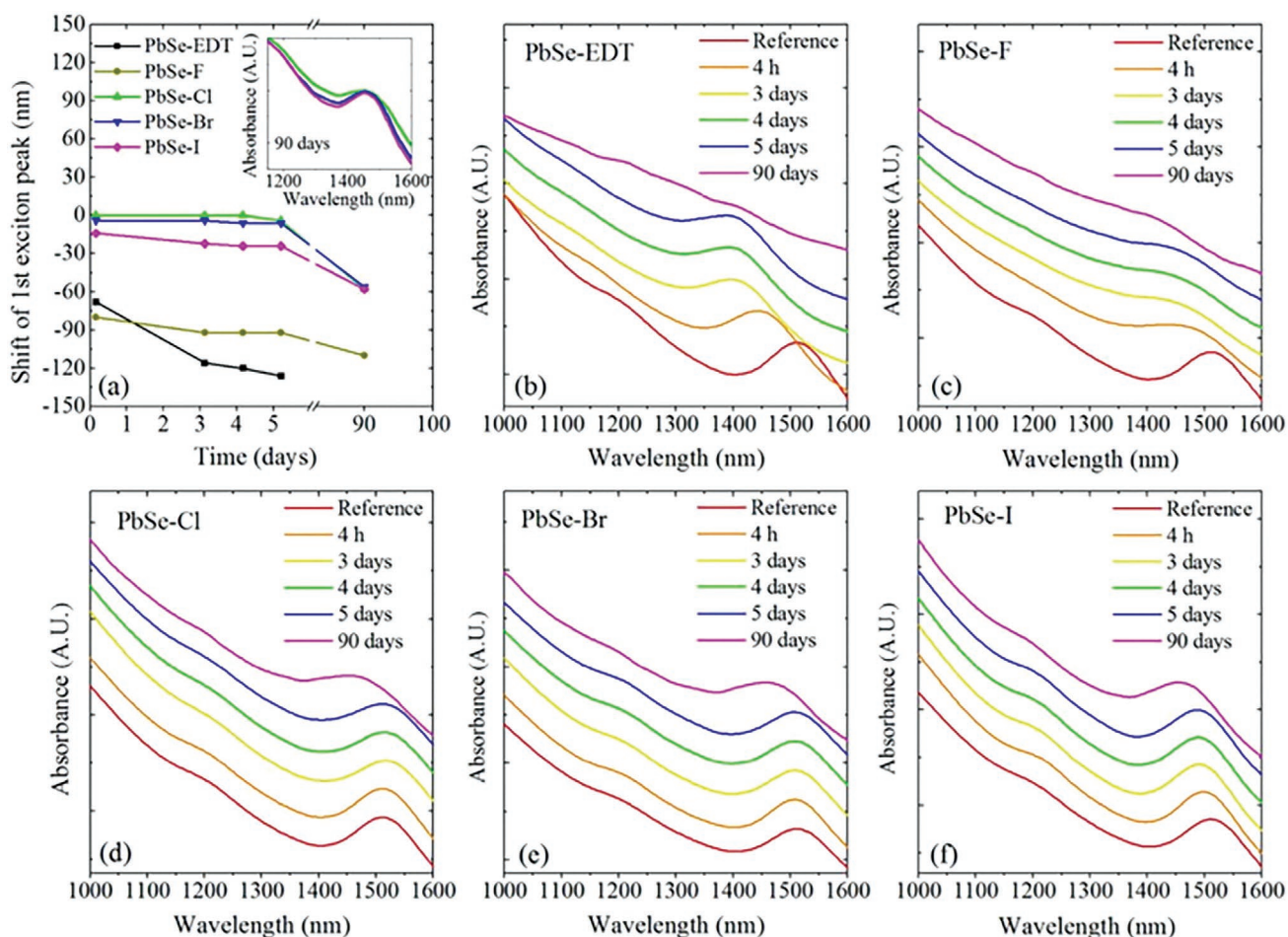


Figure 7. Time evolution of the absorbance of the PbSe QD thin films fabricated with five different ligands upon exposure to air. a) Summary of shifts in the first exciton peak position of the samples over time; the inset compares the peak width of PbSe-Cl, PbSe-Br, and PbSe-I after 90 days. Absorbance evolution of b) PbSe-EDT, c) PbSe-F, d) PbSe-Cl, e) PbSe-Br and f) PbSe-I. Reproduced with permission.^[96] Copyright 2015, American Chemical Society.

as a passivation agent.^[53] On the other hand, Cl^- , Br^- , and I^- passivated films showed only a slight blue-shift after five days, and their first excitonic peak was maintained for more than 90 days. The tetrabutylammonium iodide (TBAI)-treated films were found to be most stable, showing the lowest degrees of peak broadening and blue-shift. Zhang et al.^[97] also found that iodide led to a superior passivation in their comparison of PbSe QDSCs using TBAI, cetyltrimethylammonium bromide, EDT or 3-mercaptopropionic acid (3-MPA) as ligands. A subsequent study by Lin et al.^[69] reinforced the finding that iodide is the best halide for PbX QD passivation. In their study of solution-phase lithium halide salt passivated PbX QDs, the PbSe-LiI dots exhibited the highest photoluminescence quantum yield (PLQY). Further studies also reported iodide as a superior passivating agent. Crisp et al.^[98] found that PbI_2 gave a superior passivation to PbCl_2 , and Lan et al.^[99] showed an improved device performance with a molecular I_2 treatment. Such a superior passivation of I-treated PbX QDs as compared to other halides can be explained by hard and soft acid/base theory, which predicts that iodide has stronger bonding with Pb^{2+} than chloride or bromide.^[54,69,96] Recently, Choi et al.^[89] demonstrated that the stability of iodide-treated PbS QDs could be greatly improved by incorporating potassium iodide (KI) into the ligand exchange solution. The PbS-KI- PbI_2 device maintained 83% of its PCE after 300 h of continuous light soaking, while the PbS- PbI_2 control device dropped to 75% of its initial PCE after only 50 h. Similarly, Marshall et al.^[94] investigated PbSe solar cells treated with an assortment of metal chloride salts and found that a postsynthetic CdCl_2 treatment resulted in a larger stability improvement than treatment with chloride salts of Na^+ , K^+ , Zn^{2+} , Sn^{2+} , Cu^{2+} , or In^{3+} . The CdCl_2 -treated solar cells maintained at least 70% of their initial PCE after 200 days in air. These reports suggest that metal halides are particularly promising for passivation of PbX QDs.

PbX QD passivation is not limited to the use of halides. Woo et al.^[100] had achieved good results with oleate-capped PbSe QDs passivated by phosphonic acids.^[100] Their approach was based on simply replacing a common selenide precursor, trioctylphosphine selenide, with tris(diethylamino)phosphine selenide (TDPSe). Absorption spectra of a dispersion of passivated dots in tetrachloroethylene maintained their peak positions after three weeks in air. These dots were utilized in field-effect transistors, but this approach may also be worth exploring in the context of photovoltaic applications. Hughes et al.^[28] studied PbSe QDs passivated by an alkylselenide ligand, and found out that while short-term oxidative resistance was increased, these ligands themselves introduced additional trap states.

Selenide and telluride-based PbX QDSCs are more sensitive to oxygen than their sulfide-based counterparts, so that producing stable devices presents a far greater challenge. Better progress has been made on PbSe QDSCs than on the PbTe ones, with the former being successfully fabricated in air by Zhang et al. in 2014.^[26] Similarly to PbS QDs, PbSe QDs were passivated in situ by using various lead halides as precursors. The same group also utilized cadmium chloride for the passivation of PbSe QDSCs and established the CdSe-to-PbSe ion-exchange method, which has since been adapted by many other groups.^[29] The reported solar cells retained 66% of their photovoltaic performance after 4 days, with PCE decreasing

from an initial value of 6% down to 4%. Subsequent efforts devoted to PbSe QDSCs resulted in steady improvement in their performance and stability. It has been found that perovskites can be used postsynthesis in PbSe QDSCs as a source of halide ions,^[91,101] or as a performance-enhancing back layer.^[90] The advantage of using perovskites instead of halide salts as a source of Br^- and I^- ions is that they are less likely to cause QD agglomeration, which can then lead to long-range disorder.^[91,102] In the last few years, many studies demonstrating PbSe QD solar cells with efficiencies above 10% have been reported—all using diverse synthetic routes and surface treatments. Hu et al.^[92] reported that photovoltaic devices with I_2 -passivated PbSe QDs and a PCBM/ SnO_2 ETL can reach maximum PCE of 10.4%. Their sturdiest cell had a 9.9% PCE that retained 95% of its initial efficiency after 30 days in air. The most efficient PbSe QDSCs were reported by Ahmad et al. in 2019,^[103] with an initial PCE of 10.68%. PbSe QDs used to make those cells were first passivated in situ by Cd^{2+} and Cl^- through a cation-exchange scheme, and then further treated by a ligand exchange with PbI_2 . This double-passivation strategy yielded devices with excellent air and light stability: the best cells kept 94% of their initial efficiency after 30 days in air, and 96% of the initial PCE after 8 h of continuous light soaking.

There are only a few reports on PbTe QDSCs, probably because telluride is even more oxygen-sensitive than selenide,^[104] so that it is ostensibly more difficult to handle and to passivate it. Few available publications on PbTe QDSCs report rather low PCEs (under 2%).^[24,54] However, PbTe has a high potential for multiple exciton generation, and an EQE of 122% has been demonstrated in a PbTe QDSC.^[24] Liu et al.^[105] reported a method to reduce oxidation of oleate-capped PbTe QDs by introducing benzene derivatives to the surface, but the effectiveness of this treatment in solar cells has yet to be investigated.

To increase the stability of lead chalcogenide QDSCs, all the aforementioned improvements have to be considered in the context of a multilayered photovoltaic device stack. The various device layers are not independent and can influence the stability of each other, e.g., by material migration or chemical reactions at the interfaces. On the other hand, certain device layers can be utilized to improve device stability. For example, metal oxide extraction layers absorb ultraviolet light, which normally accelerates the material degradation.^[17] This suggests that diverse types of device architectures (for example, p-i-n vs n-i-p structures) needs to be investigated in the search for more stable solar cells. Furthermore, integration of impermeable layers or encapsulation of devices with water and oxygen repellent materials should be further studied, since they can increase the lifetime of the QDSCs.^[106]

3. Lead Halide Perovskite Quantum Dots

Lead halide perovskites have been widely investigated as active materials for solar cell applications. Perovskite-based solar cells reached a recent record efficiency of 25.5%,^[18] which places them on par with other well-established photovoltaic technologies. Perovskites are considered excellent materials for solar cells due to their direct bandgap ($E_g = 1.5\text{--}1.6$ eV),

long charge-carrier diffusion lengths and high charge carrier mobility. Colloidal nanocrystals (QDs) of lead halide perovskites offer additional benefits in terms of both phase stability and bandgap tunability.^[107] Perovskites are also often thought of as being “defect tolerant,” meaning that their intrinsic defects do not act as electron/hole trap states.^[108] This advantageous property is not observed in conventional II–VI, III–V, and IV–VI semiconductor QDs, making perovskite QDs unique in their innately low density of traps. This low density of defects renders electronic surface passivation with ligands or wider bandgap materials a less stricter requirement.^[109] While colloidal perovskite QDs exhibit significantly enhanced phase stability at room temperature in comparison with their bulk counterparts,^[110] much remains unknown about their degradation mechanisms. In fact, the long-term stability of halide perovskites and photovoltaic devices based thereon, in particularly under operation, has emerged as the most urgent problem confronting the perovskite research community. Many factors lead to the degradation of perovskite materials, such as exposure to higher temperatures, illumination, oxidizing environments, and especially to a humid environment. To tackle this issue, significant efforts have been invested by the scientific community, which have been thoroughly documented for polycrystalline thin-film perovskites elsewhere.^[111,112] In this chapter, we will discuss the current efforts to enhance the stability and durability of perovskite-based QDSCs (PeQDSCs), mainly in view of two commonly used fundamental strategies. The first one focuses on the improvement of the intrinsic stability of perovskite QD materials, which can be accomplished by i) compositional engineering, ii) producing heterostructures, iii) proper choice of perovskite QD surface ligands during the synthesis, and iv) dimensionality control. The second strategy focuses on the

optimization the PeQDSC devices in order to protect the active absorber perovskite layer from the external environment, for example, by optimizing deposition procedures and employing specific device architectures. In the following sections, the fundamental causes of degradation of perovskite QDs will be considered, and the above-mentioned strategies to overcome these pathways will be outlined.

3.1. Background and Material Properties

Perovskite QDs (PeQDs) possess a general ABX_3 stoichiometry, which is composed of a backbone of corner-sharing $[BX_6]^-$ octahedra, with cuboctahedral voids occupied by A cations, as shown in **Figure 8a**. Organic–inorganic (hybrid) halide perovskites have the following components: the monovalent A-cation is either methylammonium (MA), formamidinium (FA), or guanidinium (GA); the divalent B-cation is mostly lead (Pb), but can also be tin (Sn), or germanium (Ge); and the X-anion is chlorine, bromine, iodine, or a combination of those. All-inorganic halide perovskites differ in that their A cation is either cesium (Cs) or rubidium (Rb).

In what is often cited as the first attempt to integrate lead halide perovskites into photovoltaic devices, a material synthesized from CH_3NH_3I and PbI_2 was used as a light absorber in a titanium dioxide (TiO_2) based device with a PCE of 3.8%, as reported by Miyasaka’s group at 2009.^[113] The low efficiency of those devices was due to a low current density of the dye-sensitized architecture, which later was solved by taking advantage of the high electric conductivity of lead halide perovskite thin films. The performance of planar perovskite solar cells has since improved to a record PCE of 25.5%.^[18] Unfortunately,

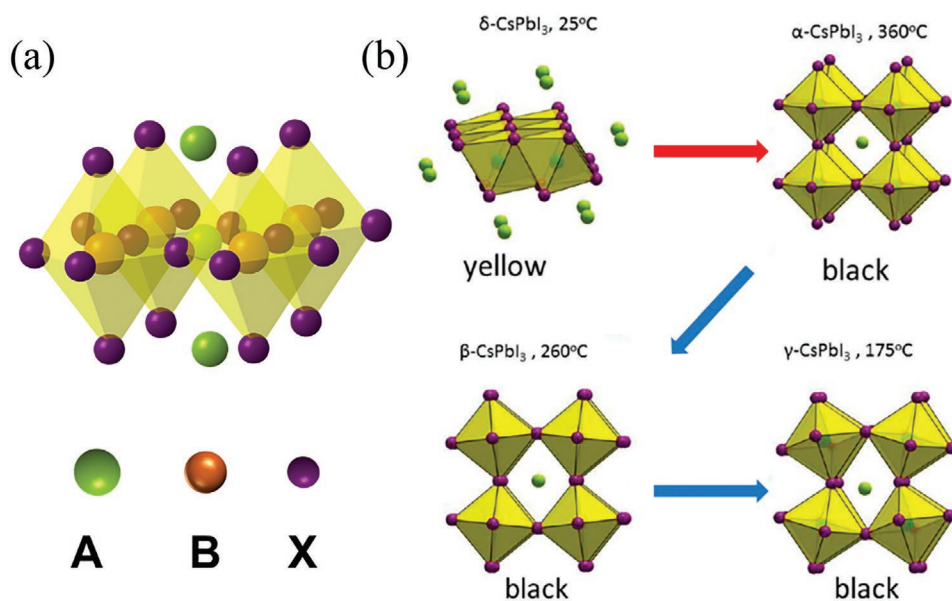


Figure 8. a) Illustration of ABX_3 crystal structure of lead halide perovskites made of corner sharing octahedra with void filling (in)organic cations. b) Thermodynamical phase transitions of $CsPbI_3$ crystals: The strongly absorbing black α -phase is the optimal one for photovoltaic applications, which has a transition temperature of 360 °C. At lower temperatures the cubic symmetry is broken and, even though the film appearance is still black, the perovskite unit cells are distorted and receive the names β - and γ -phase. The next phase, the δ -phase, transitions at 25 °C and its appearance is yellow. Reproduced with permission.^[118] Copyright 2015, American Chemical Society.

the presence of an organic cation tends to cause degradation under common external conditions, such as electric fields, moisture, photo-oxidation, and UV irradiation which trigger a nonreversible degradation process. For example, the solar cells may become transparent due to the formation of PbI_2 after the volatile MA and iodine species react under atmospheric conditions. Even prior to material decomposition, exposure to these factors may lead to the formation of defects, which act as traps and cause hysteretic effects and consequent deterioration of the photovoltaic performance.^[114]

To avoid the more unstable perovskite constituents such as MA and iodine, they may be—at least partly—replaced by other organic cations or halides. Due to the large ionic radius of iodine, the binding strength of iodides is small compared to halides with reduced radius and therefore it is more prone to migrate inside the crystal or react with the environment.^[115] For instance, FA and bromine or chlorine can be used in order to boost the stability of PeQDSCs. Alternatively, it is possible to employ a purely inorganic composition, thus eliminating the easily degradable organic components. Such inorganic perovskites, i.e., CsPbX_3 (with $X = \text{I}, \text{Br}$ or Cl), are particularly promising in terms of their thermal stability, and more importantly, can eliminate concerns about the volatility of MA. It is well-known that the crystal structure has a direct impact on device performance and is also directly linked to the absorption characteristics of the materials. CsPbX_3 crystallizes in several polymorphs in the perovskite lattice: α , β , γ , δ , as shown in Figure 8b on example of CsPbI_3 .^[116] The cubic α - CsPbI_3 black phase, which is ideal for strong light absorption in the visible range, is thermodynamically unfavorable. This black phase degrades into an undesired wider bandgap orthorhombic yellow δ -phase quickly under ambient conditions. This makes device fabrication very challenging since the δ -phase tends to form during annealing and exposure to humid ambient conditions.^[117] The black-to-yellow phase transition process can be traced back to the distortion between connected $[\text{BX}_6]^{4-}$ octahedra in the ionic crystal structure. The cubic α -phase CsPbI_3 experiences transformation to β -phase at 260 °C and γ -phase at 175 °C, exacerbating distortion between connected $[\text{BX}_6]^{4-}$ octahedra before finally reaching the δ -phase, which is in principle a successive and reversible process under stimuli of different temperature.^[118]

By reducing the size of the crystals to the nanometer regime, the reduced surface energy helps in stabilizing the CsPbX_3 perovskites in the form of PeQDs. The cubic phase of CsPbI_3 becomes more stable when the nanocrystal size is decreased.^[119] In 2016, Swarnkar et al. reported on the synthesis of a series of CsPbI_3 QDs with varying sizes (8–16 nm),^[120] using the hot-injection method adapted from early work by Protesescu et al.^[121] To incorporate these QDs in solar cells, their long, insulating ligands should be removed and this process is different in case of anionic (oleate) and cationic (oleylammonium) ligands. The former can be removed by using dry methyl acetate (MeOAc) as an antisolvent, after each layer of QDs is deposited via layer-by-layer approach leading to thin films with efficient charge transport.^[122,123] The latter can be removed by formamidine salts.^[124] Both approaches have been investigated in PeQDSCs, leading to a record efficiency of 16.6%. These devices were fabricated using a cation-exchange strategy that allowed a

controllable synthesis of $\text{Cs}_{1-x}\text{FA}_x\text{PbI}_3$ QDs across the entire compositional range ($0 \leq x \leq 1$), which is not easily accessible in polycrystalline perovskite thin films.^[10]

3.2. Compositional Engineering at the A, B, and X Sites of Perovskite Quantum Dots

The rules that govern the formation of the perovskite crystal structure were outlined by Victor Goldschmidt, who in 1926 introduced his namesake tolerance factor^[125]

$$t = \frac{r_A + r_X}{\sqrt{r_B + r_X}} \quad (1)$$

where r_A , r_B , and r_X are the ionic radii of the respective ions in the ABX_3 structure. In general, stable perovskite structures are able to form when the tolerance factor is within the range of 0.76–1.13, while other perovskite-related structures are stable outside this range. As was pointed out in the previous section, it is difficult to thermodynamically stabilize the cubic phase of perovskites. This becomes even more complicated when the void filling cations between lead halide octahedra are excessively large or small. The Goldschmidt tolerance factor can serve as an estimate guide for the choice of the correct cations for each perovskite composition. Perovskites at the edge of the tolerance factor requirement, such as FAPbI_3 ($t \sim 1$) and CsPbI_3 ($t \sim 0.8$), easily undergo a phase transition at room temperature to the more stable hexagonal and orthorhombic phases. For this reason, changing the tolerance factor by adjusting the cations and/or halides in perovskites has become an important strategy to not only tune their electronic properties, but also to enhance their stability.

One example for such a compositional engineering approach is based on the formation of mixed halide PeQDs, which can be obtained by simply mixing colloidal solutions of different compositions under ambient conditions, for example, CsPbI_3 and CsPbBr_3 QDs. The resultant mixed halide materials, such as CsPbI_2Br , exhibit superior structural stability in the cubic phase than their full-iodide CsPbI_3 counterparts. At the same time, the introduction of bromine anions in the PeQDs leads to a blueshift of their bandgap,^[126,127] making them of particular interest for either semitransparent or tandem solar cell applications. Such mixed halide compositions have been explored as active layers in solar cells, leading to high V_{OCs} of $\approx 1.3 \text{ V}$,^[126,127] and most importantly, a retention of 90% of their initial PCE after 40 days air storage without encapsulation, making them significant more stable than their CsPbI_3 counterparts. Ghosh et al. have shown that the enhancement in stability depends on the fine-tuning the iodine to bromine ratio, demonstrating that $\text{CsPbBr}_{1.5}\text{I}_{1.5}$ had superior ambient stability to CsPbI_2Br PeQDSCs.^[128] It is noteworthy, however, that light-induced halide segregation was observed in photostability tests with the consecutive loss of V_{OC} .^[129,130]

In contrast to X-site alloying, A^+ cations were shown to have the largest influence on the overall PeQD stability. For example, a partial substitution of FA by Cs via a postsynthetic cation exchange can significantly enhance the thermal stability of the PeQDs (Figure 9a). Another example is shown in Figure 9b

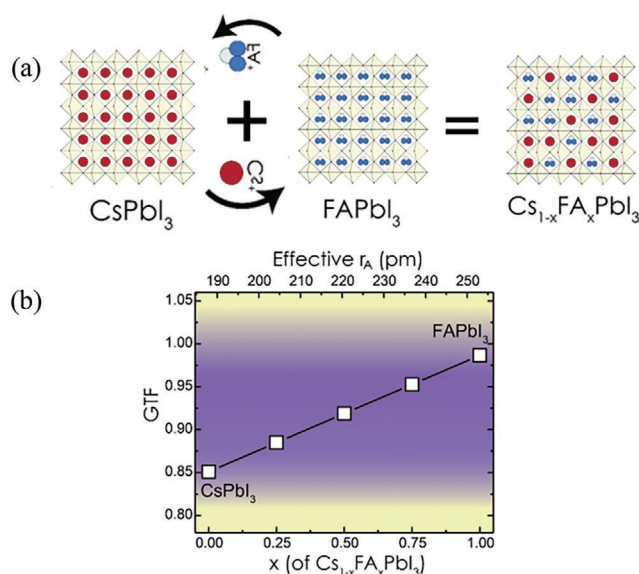


Figure 9. a) Schematic diagram showing the cross-exchange of Cs^+ and FA^+ ions between CsPbI_3 and FAPbI_3 PeQDs. b) Goldschmidt tolerance factor as a function of FA^+ ion concentration shows that all perovskite compositions are expected to be phase-stable (within the purple region of the plot). Top axis shows the effective or average A-site radius. Reproduced with permission.^[131] Copyright 2018, American Chemical Society.

that demonstrates how the Goldschmidt tolerance factor can be tuned by changing the composition of $\text{Cs}_{1-x}\text{FA}_x\text{I}_3$ PeQDs. Correspondingly, the cubic phase of CsPbI_3 QDs can be stabilized upon addition of FA cations to the nanocrystals which yield not only efficient, but more importantly, air-stable devices under room temperature.^[10,131]

Metal ion doping at the B site of perovskite QDs represents yet another effective route to tune their stability and is additionally motivated by the possibility to replace the toxic lead in PeQDs. However, one should be aware that the substitution of Pb cation is more difficult than ions at the A- and X-sites, since the B cation directly determines the size of $[\text{BX}_6]^{4-}$ unit cell. This can trigger the tilting of neighboring $[\text{BX}_6]^{4-}$ octahedra and generate an undesired lattice strain. There have been several reported attempts to dope perovskite QDs by incorporating isovalent cations (e.g., Sn^{2+} , Mn^{2+} , Sr^{2+} , Cd^{2+} , Ca^{2+} , Zn^{2+} , Ge^{2+}),^[132–142] with the goal of improving both luminescence efficiency and stability. However, the majority of these studies stopped at colloidal solutions as their final step, or the PeQDs were utilized solely in LEDs. Improved structural stability via B-site doping in PeQDSCs has been demonstrated only in a few cases. For example, Mn^{2+} doped CsPbCl_3 PeQDs were used as an energy-down-shift layer in planar perovskite solar cells for an increased performance and stability.^[137] Using GeI_2 together with PbI_2 resulted in a Pb-depleted and iodide-rich surface environment, which enhanced both the colloidal and the photovoltaic stability.^[138] Shi et al. stabilized CsPbI_3 QDs with the assistance of guanidinium (GA^+), which was previously considered too large for the 3D perovskite structure.^[143] Consequently, the GA-matrix-confined CsPbI_3 QDs exhibited remarkably high charge mobility and diffusion length as compared to the undoped CsPbI_3 QDs, leading to photovoltaic devices with a

maximum efficiency of 15.2%.^[144] Therefore, tailoring the structural stability of PeQDs by incorporation of suitable dopants remains a topic with high potential.

3.3. Heterostructures

Heterostructured nanocrystals often consist of a core and a protective shell with many well-known examples such as CdSe/CdS core-shell structures.^[145,146] However, the formation of core-shell nanocrystals based on PeQD cores is complicated, due to the need to create a heterostructure between an ionic crystal (perovskite) and an atomic crystal (alloy semiconductor).^[147] Still, such structures can be designed as is illustrated by the example of $\text{CsPbI}_3/\text{Mg}_x\text{Zn}_{1-x}\text{Te}$ QDs proposed by Zhang et al.^[147] It is expected that such heterostructures can prevent ion migration inside the PeQD solid when an electric bias is applied at the outer electrodes, thus enhancing their stability.

On the other hand, the excellent match in the lattice constants of lead chalcogenides with those of perovskites offers the possibility to form a range of core-shell heterostructures. As an example, the lattice matching of the crystal structures of MAPbI_3 and PbS is shown in Figure 10a,b.^[148] Such core-shell PbS-perovskite structures can be easily fabricated in solution and have been shown to enhance both the performance and stability of solar cells.^[149,73] At the same time, examples of core-shell heterostructures with perovskite QDs as the core material remain scarce. $\text{CsPbI}_3/\text{PbSe}$ heterostructured QDs were directly synthesized in a colloidal phase using trioctylphosphine selenide as a Se source.^[150] TEM and HRTEM images in Figure 10c,d show a central area marked by an interplanar distance of 0.62 nm, which was identified as CsPbI_3 QDs. The surface region in these images was identified as PbSe , with an interplanar distance of 0.3 nm associated with its (200) plane. Solar cells based on these $\text{CsPbI}_3/\text{PbSe}$ QDs not only reached a respectable PCE of 13.9%, but also showed a significantly enhanced storage stability in humid environments. The devices retained 80% of their initial PCE after 60 h of storage in air, while reference CsPbI_3 -based devices maintained only 50%.

Yet another promising protective semiconductor material is ZnS , whose crystal structure matches well with that of PeQDs. The use of ZnS as a shell was reported to prolong the PL lifetime of CsPbBr_3 NCs from 13 to 106 ns.^[151] In terms of stability, films processed from $\text{CsPbBr}_3/\text{ZnS}$ QDs maintain PL intensity for more than 2 days whilst immersed in water, whereas the PL of films made from CsPbBr_3 QDs was completely quenched within 2 h. While this result is promising, such heterostructures have not yet been investigated in the context of photovoltaic applications.

3.4. In Situ Surface Ligand Exchange

Oleic acid and oleylamine are two commonly utilized bonding ligands in colloidal synthesis of PeQDs, as they enable their growth in a wide range of organic solvents. Unfortunately, these ligands with long alkyl chains are electronically insulating, producing a tunneling barrier between neighboring QDs and between the QD layer and the outer electrodes. In practice,

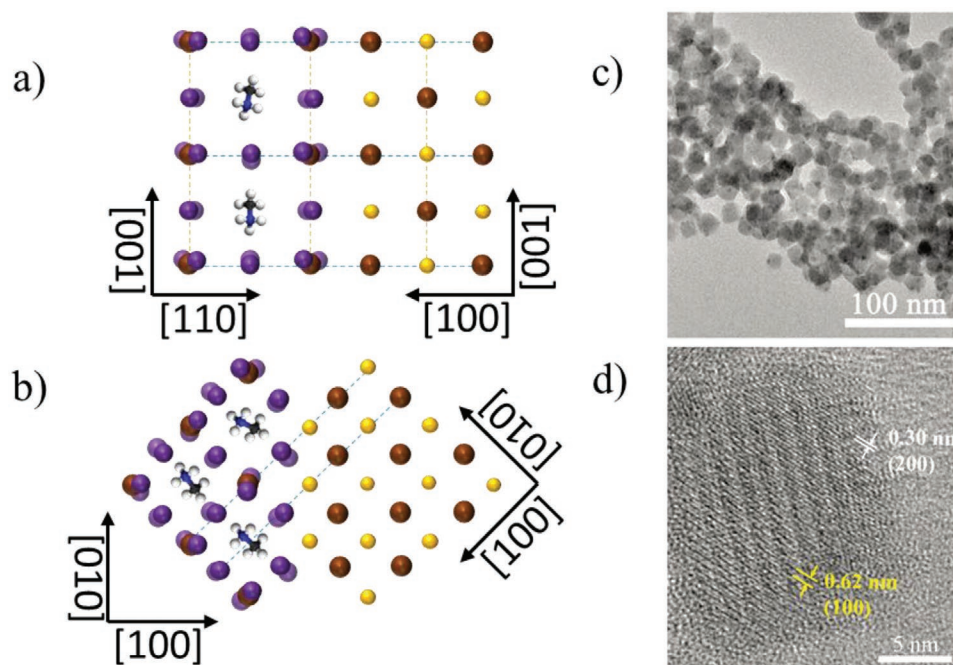


Figure 10. a,b) Crystal structure model demonstrating the lattice matching between MAPbI₃ and PbS. c) TEM and d) HRTEM images of CsPbI₃/PbSe heterostructured NCs. Reproduced with permission.^[150] Copyright 2020, American Chemical Society.

surface ligand modification of PeQDs is not as straightforward as ligand exchange in traditional II–VI or IV–VI QDs.^[152] Most conventional methods result in structural transformation or loss of binding motives in PeQDs due to their highly ionic nature.^[153] One of the biggest challenges in the fabrication of stable and conductive perovskite QDs films is to strike the balance between QD dispersity and adhesive forces by properly modifying their native surface ligands. This can be achieved both by ligand engineering during the PeQD synthesis, and by ligand exchange performed on the PeQD films.

Shortening the length of the PeQD ligands is a simple and effective method to achieve enhanced carrier charge mobility and stability. In their fabrication of CsPbI₃ QDs, Chen et al. partially replaced oleic acid, which includes 18 carbon atoms, with octanoic acid, which contains only 8 carbon atoms; these were coordinated with octylamine as cocapping ligands.^[154] The resulting PeQDs had increased PLQY from 80% ± 6% to 94% ± 3% and enhanced PL stability, maintaining 80% of the initial PL intensity after 180 days. Unfortunately, although their CsPbI₃ QDs based solar cells were demonstrated to achieve a high PCE of 11.87%, no stability studies were reported. Another effective short ligand is phenyltrimethylammonium bromide (PTABr), which endows CsPbI₃ QD based solar cells with better performance and enhanced stability in three ways. First, PTABr ligands with a short benzene group can lower the repelling force between QDs during film formation, and hence facilitate charge carrier transport. Second, the Br moiety passivates the iodine ion defects, which is consistent with reports that an iodide-rich surface environment results in more stable perovskite QDs. Finally, PTABr ligands can increase the resistance against water induced degradation due to the hydrophobicity of PTABr-CsPbI₃ films. Consequently, PTABr-CsPbI₃ devices

maintained 80% of their initial PCE in ambient conditions for one month without any encapsulation.^[138]

3.5. Dimensionality Control

The most common structure of perovskite QDs remains the 3D ABX₃ crystal structure and composition, consisting of a network of corner-sharing PbI₆ octahedra with void-filling A cations. When long-chain organic cations such as butyl-ammonium (BA) or phenethylammonium (PEA) are used as A-cations, the 3D perovskite structure will become layered, forming so-called 2D or quasi-2D structures.^[155–157] As is shown in **Figure 11a**, the layers with thickness (*n*) are subsequently reduced in size and exhibit a strong quantum confinement effect. Their increased formation energy should therefore improve the material stability as well as device stability. To examine this, Quan et al. compared the stability of 2D perovskite materials with different layer numbers (*n* value).^[161] These layered perovskites were tracked by XRD during storage at 90% relative humidity for a period of one week. Unlike for 3D perovskites, the XRD peak intensity of 2D perovskite films showed no obvious changes, indicating a significantly improved stability. However, there is a trade-off between stability and performance as is shown in **Figure 11c**, since the long-chained A-cations serve as insulating barriers which prevent charge transport and extraction from the perovskite sheets. Higher performance, albeit a lower stability, was observed while increasing the number of layers *n* in (PEA)₂(MA)_{*n*}Pb_{*n*}I_{3*n*+1} perovskites. Quan et al. found that *n* = 60 quasi-2D perovskite based solar cells achieved an optimal counterpoise between stability and performance, presenting a hysteresis-free certified AM1.5 PCE of 15.3%.^[161]

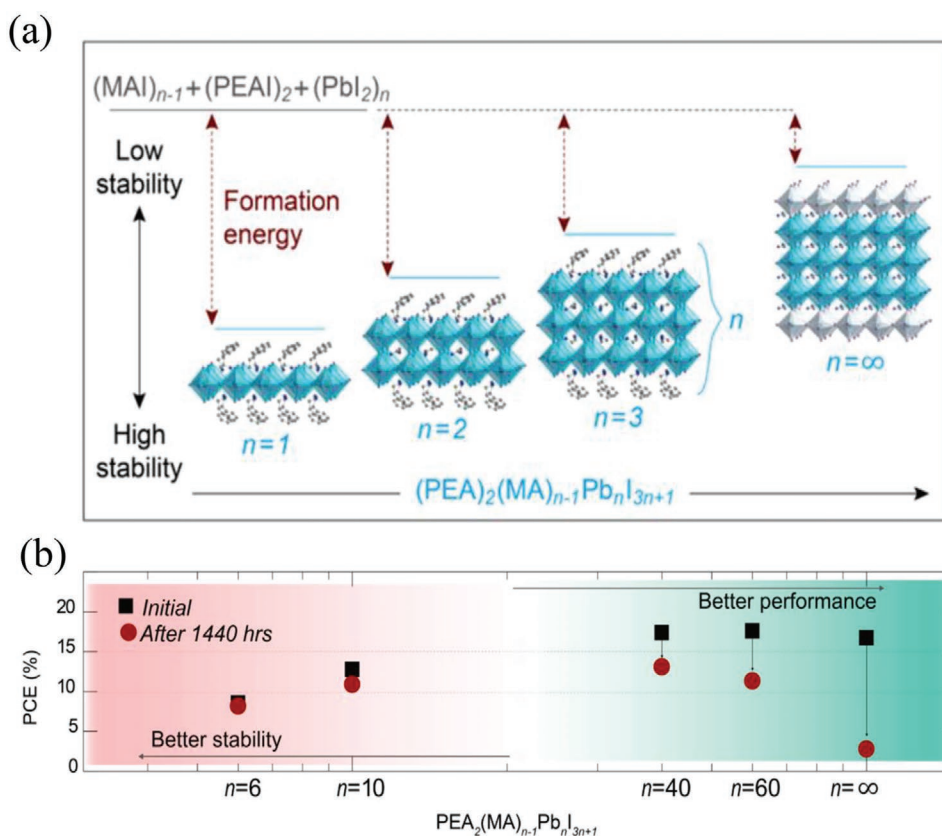


Figure 11. a) Unit cell structure of $(\text{PEA})_2(\text{MA})_{n-1}\text{PbI}_{3n+1}$ perovskites with different n values, showing the evolution of dimensionality from 2D ($n = 1$) to 3D ($n = \infty$). b) PCE of solar cells based on layered $(\text{PEA})_2(\text{MA})_{n-1}\text{PbI}_{3n+1}$ perovskites as a function of n value, which shows that increased performance was achieved with an increased n value; however, stability was decreased. Reproduced with permission.^[161] Copyright 2016, American Chemical Society.

Using additives such as phosphine oxides can further enhance the stability of perovskites with reduced dimensionality by passivating their exposed surfaces.^[158] Mixed-dimensional perovskites (0D, 1D, 2D, and 3D) as absorber layers can be employed to find an optimal point for stable and efficient solar devices. Zhang et al. fabricated solar cells with nanostructured perovskite heterojunctions formed by 0D QDs, 2D nanosheets, and 3D bulk CsPbBrI_2 perovskite in a gradient layer-by-layer architecture.^[159] Such an architecture has been shown to result in favorable energy band alignment, resulting in an increased photocurrent. The dark storage and operational stability (25 °C at 35% relative humidity) were both significantly improved for the 3D–2D–0D mixed solar cells.

3.6. Lifetime-Enhancement Strategies for Perovskite Quantum Dot Solar Cells

Solar cells based on perovskite QDs are relatively new, having been first introduced by the Luther group in 2016 who reported CsPbI_3 QD devices with a respectable PCE of 13.43 %.^[120,160] In 2019, Hao et al. reported on the current certified efficiency record for PeQDSCs fabricated using hybrid $\text{Cs}_{0.5}\text{FA}_{0.5}\text{PbI}_3$ QDs reaching a PCE of 16.6 %, ^[10] which translates into a relative improvement of 123% in efficiency achieved within just three years. Other perovskite compositions have also been explored.

For example, there have been reports investigating CsPbBr_3 or CsPbBrI_2 PeQDSCs, however due to the larger bandgaps, their performance was relatively low.^[126,161] Hybrid organic-inorganic perovskite compositions such as FAPbI_3 QDs have also been employed as photoactive absorbers in devices, either on their own or in combination with CsPbI_3 QDs.^[10,123,162]

The vast majority of PeQDSC reported in literature share several common features. The most-often used active material is CsPbI_3 QDs since its bandgap is well-suited for absorbing solar wavelengths, resulting in a higher photocurrent. Another similarity is the device architecture. Most devices utilize transparent TiO_2 or SnO_2 ETLs, with films of 2,2',7,7'-Tetrakis[*N,N*-di(4-methoxyphenyl)amino]-9,9'-spirobifluorene (Spiro-OMeTAD) or other organic molecules serving as HTLs. The preferential contacts used for these devices are Ag or Au electrodes, sometimes with a thin MoO_3 layer. These devices can be assembled in air as long as the relative humidity in the lab does not surpass 20%.^[160]

PeQDSCs are usually tested without encapsulation in either air or nitrogen. For example, CsPbI_3 QDSCs maintained 98% of their starting PCE after one month of storage in a nitrogen-filled glovebox,^[163] but when the same devices were exposed to 60% relative humidity, their PCE lost 90% of the initial value due to QD decomposition. Showing an improved stability, CsPb(I/Br)_3 devices maintained 90% of their initial performance after 900 h of storage in a dry glovebox.^[126] Thermal

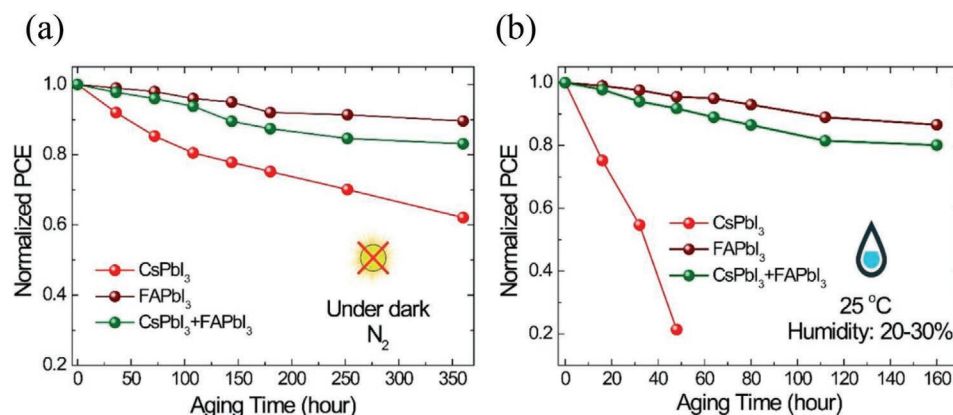


Figure 12. Lifetime of PeQDSCs with fully inorganic CsPbI₃ and mixed organic/inorganic FAPbI₃ PeQDs under a) nitrogen without illumination and b) humid air and room temperature. PeQDSCs made of FAPbI₃ perovskite are more stable than the inorganic counterpart and a mixture of both dots follows the stability pattern of the more stable devices. Reproduced with permission.^[162] Copyright 2019, American Chemical Society.

stability has also been investigated, with only 3 h at 100 °C causing a major loss in performance, associated with the transition of the CsPbI₃ QDs to their orthorhombic phase.^[163,164]

Wide-bandgap PeQDs, such as CsPbCl₃, have shown promise for energy down-shifting in MAPbI₃ solar cells. The PeQD layer absorbed UV light and thus slowed down the degradation process of the underlying perovskite layer. Solar cells made using this approach were stable for 100 h illumination in a nitrogen atmosphere.^[137]

Several approaches have been shown to enhance the device stability of PeQDSCs. For example, the use of mixed CsPbI₃ and FAPbI₃ QDs was shown to result in more stable devices than their all-inorganic counterparts, since FAPbI₃ QDs are more stable as is shown in **Figure 12**.^[123] This increase in stability is already evident in a nitrogen atmosphere, but becomes significantly more pronounced when the devices are exposed to humid air conditions. It has been also reported that mixing these two types of perovskite QDs prevented the conversion of CsPbI₃ QDs from the cubic α -phase to the δ -phase by lattice contraction effects.^[162]

An alternative approach is based on the use of dopants or additives. For example, Cs-salt doping (e.g., with Cs acetate) of CsPbI₃ QD films were shown to enhance the solar cell stability in air by filling the Cs vacancies at the QDs' surfaces.^[165] Other doping strategies such as incorporation of GeI₂ or PbI₂ also resulted in an enhanced shelf life of CsPbI₃ QDSCs. These devices maintained their initial performance after 80 days in a dry environment.^[138] Alternatively, ytterbium doping has also been proposed as an effective defect passivation strategy for perovskite QDSCs, leading to an enhanced stability of solar cells operated in humid air.^[134]

The method by which PeQDSCs are fabricated may directly affect their operational stability. It has been mentioned already that the humidity during fabrication should not surpass 20%. Another aspect is the sequence in deposition of PeQD layers: if it is applied in a single step, the stability can be enhanced as compared to a layer-by-layer deposition, because washing steps that follow the deposition of each layer may introduce defects in the PeQD films and serve as additional pathways for degradation.^[127] It has also been shown that cross-linking the CsPbI₃

QD films using μ -graphene could improve their stability even in hot and humid environments, largely due to the prevention of QD agglomeration.^[163]

The choice of the organic HTL layer in QDSCs can also strongly influence the overall stability of the device. Most of the high performing PeQDSCs employ Spiro-OMeTAD as HTL—a well-known cause of degradation in perovskite photovoltaics. One example of a promising substitute to Spiro-OMeTAD is poly[[4,8-bis[(2-ethylhexyl)oxy]benzo[1,2-b:4,5-b']dithiophene-2,6-diyl][3-fluoro-2-[(2-ethylhexyl)carbonyl]thieno[3,4-b]thiophenediyl]] (PTB7), which has been shown to improve the stability of the devices,^[164] however other alternatives need to be investigated to enhance the stability further.

4. Lead-Free Quantum Dot Photovoltaics

The previous sections have focused on assessing the stability of lead-based QDs and QDSCs. This section will cover stability of some other types of QD materials used in photovoltaics, namely those that do not contain lead. Generally speaking, solar cells can be made of any type of semiconducting material as long as its absorption is congruent with the solar spectrum. Correspondingly, many choices and combinations of QD materials have been reported in literature, and it would be beyond the scope of this review to discuss and describe all of them. We refer the readers to other existing reviews on this topic.^[166,167] We thus chose to focus on some selected examples of lead-free nanocrystals such as binary like CdSe and InP, and tertiary compounds like AgBiS₂.^[168–170] The highest reported PCEs of solar cells made from these types of QDs are currently around 13%,^[171] while there is a push toward further optimization that may yield higher values in the coming years. Even though the material compositions used in these solar cells are different to those discussed in the previous sections, most of the device architectures are similar, making the comparison of degradation processes possible.

CdSe QDs have been extremely well studied for their potential as luminescent materials in LEDs and as fluorescent biomarkers.^[5,172] This type of QDs has been generally shown to be stable both in colloidal solutions and in solid films, in

particular in terms of their colloidal stability and photostability, with significantly fewer studies examining the stability of their optoelectronic properties, mechanical or thermal stability. In the following section, we will summarize some of those observations and findings. Moreover, we will also outline the recent progress in other promising QD solar cells, such as CdTe/CdSe and CdS/CdSe hybrids, InP, and AgBiS₂ QDs.^[168,169,173,174]

4.1. Degradation Mechanisms of Colloids and Films

Colloidal stability has been extensively studied for the luminescent CdSe-core based core-shell QDs (with CdSe/ZnS been most prominent example), since their prevalent use as biomarkers. It has been shown that the pH value of aqueous solutions can influence the formation of their agglomerates.^[175] A very low concentration of dots in solution is detrimental because it facilitates deattachment of ligands from their surface. On the other hand, if their concentration is too high, the formation of agglomerates is accelerated. Yet, it is possible to obtain colloidal solutions of these QDs that are stable for over a year without any noticeable aggregate formation.^[176] The content of other ionic species in the solution might also affect the colloidal stability, as they can remove ligands from the QDs surface.^[177] The stability is not only related to the medium in which the QDs are dispersed, but is also strongly linked to the choice of ligands. Thiol and dithiol ligands have been shown to form covalent bonds to the surface of II–VI semiconductors.^[178,179] However, monothiols can detach more easily from the surface than dithiols, so that the use of the latter may help to avoid the agglomerate formation.^[180–182]

The PL stability of core-shell CdSe based QDs has been comprehensively studied in the context of bio-imaging applications, mostly with a focus on the PL of their colloidal solutions. Since QDs may undergo some structural and compositional changes under prolonged illumination, their PL intensity and also the PL peak positions may also vary with time. At this point it becomes important in which (inert or not) atmosphere the QDs are kept, as the presence of oxygen can play a major role in the degradation dynamics, as it can promote the formation of oxides on the surface of QDs. Indeed, when colloidal solutions of QDs are kept under nitrogen atmosphere, or encapsulated in an airtight cuvette, their PL signal remains stable.^[183] However, the intensity of the PL peak was increased when the QDs were exposed to air for a short period, since ambient oxygen initially passivates some of the trap states found on the dot surface, similar to what has been described earlier for PbS QDs.^[184] Extended storage of their solutions in air may lead to a complete oxidation of their surface atoms, evidenced by X-ray photoemission spectroscopy analysis that revealed the formation of SeO₂. Such formation of SeO₂ species is associated with the preferential binding of ligands to the Cd atoms instead of the Se, leaving those sites more vulnerable to oxidative attack. The size of the QDs determines the ratio of Cd to Se atoms on the surface, thereby affecting the degree of oxidation.^[185]

The PL peak of QD solutions illuminated in air for a continuous period of time may undergo a blueshift and photobleaching.^[184] A blueshift on the order of 10–40 nm has been reported for CdSe/ZnS core-shell QDs,^[184,186,187] caused

by an effective size reduction of the QD core due to photooxidation, thus enhancing the effects of electron confinement. The oxidation of the surface is accelerated by UV light exposure, which facilitates the above-mentioned oxidation processes. Once the QD surface is fully oxidized, the PL signal can vanish completely. The broadening of the PL spectra can occur due to the gradual loss of ligands and the subsequent particle agglomeration. We note that the power density of the UV light employed in these studies was higher than that of the solar spectrum, (e.g., 20 kW cm⁻² in the study by Van Sark et al.^[184]), and therefore photodegradation studies carried out using solar illumination (100 mW cm⁻²) show rather diminished effect of photo-oxidation on those QDs. The PL intensity can even be initially boosted upon exposure to sunlight due to the surface passivation. On a microscopic scale, the photodegradation of these QDs usually starts at defect sites at their surface, where dangling bonds, incomplete ligand coverage or grain boundaries may all act as centers for photooxidation.^[184,188] A comparison of core-only and core-shell QDs with different shell thickness, reveals that the former experience faster photobleaching, whereas core-shell QDs with moderate shell thicknesses show a rather stable PL, but for very thick shells the interface strain increases, thus resulting in more defects and the acceleration of degradation.^[189] Photooxidation of QDs can also be followed by changes of the PL lifetimes, as the dynamics of electron and hole recombination will significantly change due to the surface oxidation. Very often, PL decays of colloidal QDs exhibit a fast component associated with recombination in the QD core and a slow component, related to recombination via surface states. Oxidation mostly influences the surface related recombination dynamics, which also reinforces the general understanding that surface defects play a major role in the process of QD degradation.^[190]

Similar to the prototypical CdSe, other II–VI core QD materials such as CdSe and CdTe also show decreased PL signal due to agglomeration or photooxidation, with CdTe QDs being most sensitive in this respect.^[191–192] Similar trends were reported for III–V QDs such as InP with promising routes for their stabilization using a ZnSeS shell.^[193]

Exposure to heat could also reduce the PL intensity of such QDs, which is partly related to the removal of surface ligands at elevated temperatures.^[194,195] It has been shown that thick protective shells can help to enhance their thermal stability.^[196] Alternatively, doping of the shell material with Mn²⁺ ions could enhance thermal stability of QDs by passivating defect states.^[196]

Degradation processes of QDs in films are somewhat different from those in colloidal solutions. The ligands are not so easily removed from the surface in a solvent-free environment, and the dot packing is dense, enhancing cooperative effects such as energy and charge transfer inside the film, thus altering the degradation pathways.^[197] Another obvious difference is that the absolute PLQY of the QD films is typically lower than the one measured for the same QDs in solution. The degradation of films in an aqueous environment will be affected by penetration of water molecules to the core–ligand interface and will result in luminescence losses. This kinetic process can be especially damaging if the ligand density is low or the bond strength is not sufficiently high.^[198] Still, an initial increase

of the PL intensity may occur when films are illuminated in a moist environment, which could be linked to the adsorption of water molecules to the outmost atomic layer of CdSe, thus passivating the nonligated surface sites.^[199] Similarly to colloidal solutions, QD films illuminated for a prolonged time in an oxygenated atmosphere may show a blueshift of their PL spectra linked to the photooxidation of the QDs' surfaces.^[199] Again, it is important to note that during the fabrication of QD films for solar cell applications, the original long-chain ligands of colloidal QDs are replaced by short ones (such as halide ions or thiol-containing molecules) in order to allow for efficient charge transport, and this change may influence the possible degradation pathways.

The reduction of the PL signal of QDs does not necessarily imply a direct loss in absorption, which is a characteristic more relevant to solar harvesting applications. Still, the chemical degradation processes shortly summarized in this section provide valuable information that can be useful also for photovoltaic devices. For instance, the results of spectroscopic studies would still be applicable for QDs integrated in solar devices: if the PL signal is completely quenched because of the high amount of generated sub-bandgap states, the nonradiative recombination of excitons would diminish the performance of photovoltaic devices.

4.2. Device Degradation and Stability Enhancement

Solar cells made from a variety of Pb-free QDs have been reported by diverse research groups, which offer the possibility to gain further insights on device stability. Most of the studies reported on the shelf stability, i.e., the evolution in the performance of devices stored in air without illumination over a period of time. The shelf stability of CdSe QDSCs has been reported to be rather poor, with a sharp decrease in performance after relatively short periods (e.g., 80% loss after 3 days).^[200,201] The stability was further reduced when the performance of the devices was tracked under continuous illumination. For example, CdSe QDSCs showed a decrease of 25% in PCE after only 200 s of irradiation, while an additional ZnS/ZnSe shelling could improve their stability to nearly no loss in PCE over a span of minutes.^[201]

Several examples of hybrid QD solar cells, based on combinations of two II–VI semiconductor materials (e.g., CdSe/CdTe, CdS/CdTe, or CdS/CdSe), yielded better stabilities than CdSe QDs alone, reaching several hours under constant illumination and up to 6 months for storage in the dark.^[168,171] It was found that Mn²⁺ doping of QDs was an effective way to boost both performance and stability^[168,196] When Mn²⁺ ions are present at the shell of these QDs, they generate in-band states which boost the charge extraction by reducing the recombination rate at the core–shell interface.^[202] CdTe QDSCs with PCE of 12.3% were reported by Panthani et al., with an efficiency decreasing by 25% after one day illumination. This degradation could be reversed by a current/light soaking treatment.^[203]

QDSCs based on environmentally-friendly AgBiS₂ QDs possess a strong visible-through-IR absorption,^[174] and were shown to be stable in air for a period of one to three weeks. After that, degradation occurred within the organic transport layers, such

as poly(3-hexylthiophene-2,5-diyl) (P3HT) or PTB7.^[170,174] Other Cd-free QDs, such as InP or Sn-doped InP were reported to be less stable when employed in solar cell devices, showing noticeable decrease in performance after only 15 min of illumination.^[169]

Several methods to improve the stability of lead-free QDSCs have been explored. For example, optimizing the composition of the shell material of QDs in order to decrease the lattice mismatch between the core and the shell has been shown to be important for the QD stability.^[201,204] Another method involves deposition of thin layers of ZnS on top of the photoactive layer, which helps to prevent oxidation.^[200] Charge extraction layers also play a role in device stability. Electron extraction (e.g., with a TiO₂ layer) can enhance the anodic corrosion of CdSe QDs by an excess of holes, which calls for an efficient hole extracting material that compensates for the reduced hole mobility in the QD films.^[205]

Since degradation is often a QD-surface related issue, their stability could be improved by a suitable ligand passivation. As was already mentioned above, when used for device fabrication, QDs are typically treated with short chain ligands in order to improve the conductivity through the film and facilitate interdot charge transfer. Passivating the QDs' surface with thiols, though promising in terms of improving their PLQY, has been shown to lower their stability due to the detachment of thiols in colloidal solutions, especially in case when water molecules could penetrate into the core–ligand interface.^[179,192] On the other hand, passivating QDs with electron-rich ligands that exhibit strong hole-extraction ability can increase their stability.^[198] The length of the ligands needs to be carefully considered and optimized: while very short ligands might outperform longer ones in terms of improved conductivity and thus offer higher initial efficiency, longer-chain ligands typically yield more stable dots. The nature of the ligand molecules is also important, with aliphatic ligands known to be more stable than aromatic ones.^[179] Finally, the type of bond between the QD surface and the ligand also affects the stability—bidentate ligands may degrade faster than monodentate ones.^[179]

Fabrication procedures of Pb-free QD devices may also influence their stability. For example, "over-washing" of QDs after synthesis can remove too many longer-chain ligands, which results in less-stable devices.^[187,206] Fabricating devices in an inert atmosphere (e.g., in a glovebox) will yield higher absolute efficiencies for the tested cells, but will not directly improve their degradation dynamics once there are placed in air.^[200] It is also possible to encapsulate the devices after fabrication to prevent oxidation, e.g., by using thermoplastic spacers;^[173] still, penetration of oxygen cannot be completely prevented, and the devices may eventually degrade.

5. Suggestions on Stability Testing in the Quantum Dot Photovoltaic Community

One motivation for this review arised from the observation that stability testing of QDSCs is somewhat left aside when new record efficiencies are published. Relatively few publications deal directly with the topic of QDSC stability and propose strategies for its enhancement. **Figure 13** includes several

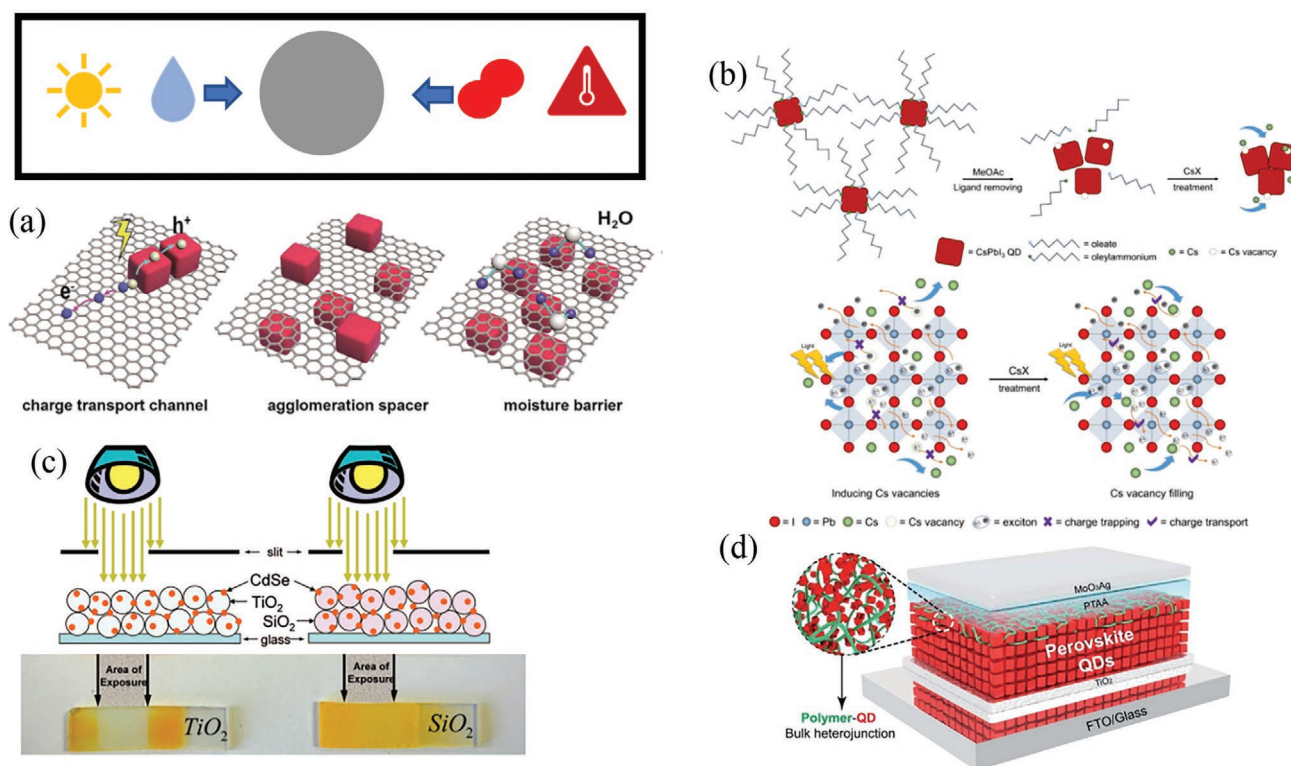


Figure 13. QD solar cells can be exposed to several stress factors during the operation, some of which are sketched in the top left panel. On the right, different strategies for QDSC stability enhancement are presented. a) Use of a thin layer of graphene as moisture and agglomeration barrier. Reproduced with permission.^[163] Copyright 2018, John Wiley and Sons. b) Passivation of QDs, for example, with cesium ions, results in a higher stability against oxidation. Reproduced with permission.^[165] Copyright 2019, John Wiley and Sons. c) Electron transport layers can enhance the QD film degradation, as is the case for titanium dioxide substrates. Reproduced with permission.^[205] Copyright 2009, American Chemical Society. d) Similarly, an organic spacer can protect the underlying layer of QDs. Reproduced with permission.^[207] Copyright 2020, The Royal Society of Chemistry.

exemplary sketches taken from those publications, which show a few of the proposed methods for improving the stability of these emerging photovoltaic materials. The degradation mechanisms can be easily extracted from a simple sketch and help the readers in understanding the overall message of the newly developed methods.

At the same time, our examination of the available body of literature related to the stability aspects of QDSC revealed the absence of a consistent and standardized method to quantify the results. To illustrate this point, we have summarized the efficiency, the conditions of stability tests, and the reported stability data on PbS QDs and PeQDs based solar cells from a selection of representative publications that appeared between 2008–2020 (**Figure 14**). While a remarkable progress in increasing the PCE of devices has been achieved, it is hardly possible to observe any clear trend in enhancing stability of those devices. As a matter of fact, the vast majority of studies reported on the ambient stability of devices in the dark, i.e., their shelf stability; assessed devices that were stored in the lab without illumination and were periodically re-measured. While the shelf stability is an important “snapshot” characteristic, evaluating the performance evolution of solar cells under operational conditions is understandably much more useful.

Surprisingly enough, even similar degradation conditions seem to lead to very different results. This could be related

to the different levels of humidity of the ambient air in different laboratories, or the different frequency of measurements during which the devices were exposed to illumination. Such a lack of consistency makes it nearly impossible to compare the results and to draw reliable conclusions on the influences of different aspects (e.g., passivation, device architecture, etc.) on the stability of the devices. Moreover, this raises questions regarding experimental reproducibility, since experiments performed at different times of the year would inevitably vary in the level of humidity.

Thus, with the common goal of increasing the device stability, the field of QDSCs would greatly benefit from a simple, standardized method for testing stability of such solar cells. In what follows, we do not intend to mimic the industrial standard, which already exists for the solar cell testing,^[214] but rather to encourage researchers active in the QDSC field to adopt a more consistent protocol for degradation characterization, which would allow for direct comparison of stability of such devices. This was recently done in the field of lead halide perovskite solar cells,^[215] and in **Table 1** we include two suggestions that could be adopted for QDSC stability testing. The first test is the so-called “stress-free test” which represents the best-case scenario for the stability of the devices. The second, “realistic test” was chosen such that the atmosphere, temperature, illumination (power), and bias voltage are close to real operational conditions.

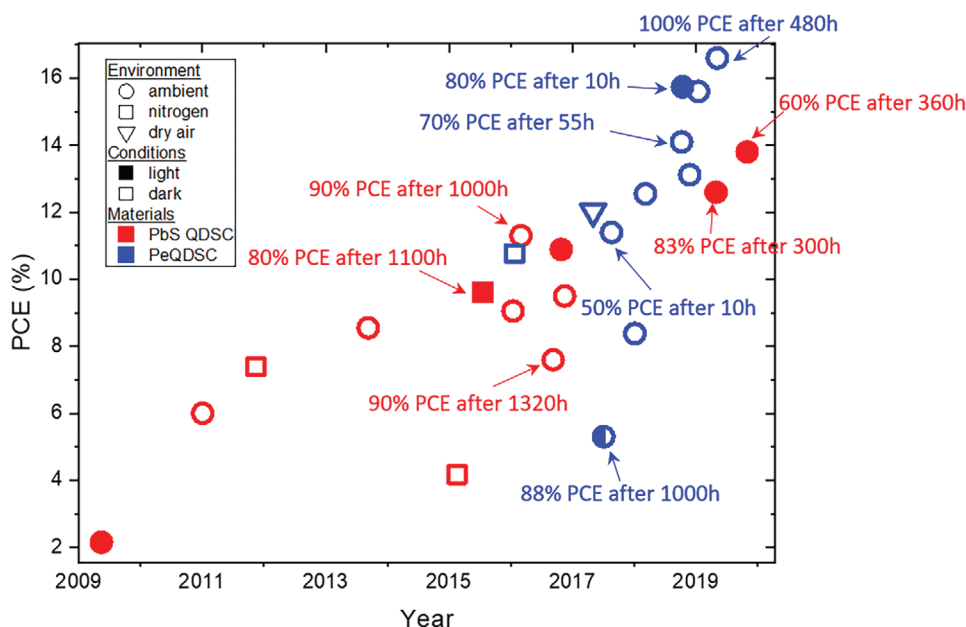


Figure 14. Evolution of PCE of PbS QD and PeQD based solar cells taken from representative publications (appeared between 2008–2020) that reported on the stability of the devices. Selected information on the retained percentage of the device's PCE, and the conditions of tests are also provided in order to illustrate the inconsistency both in the degradation conditions and duration of tests. The data points are taken from diverse publications and classified depending on the degradation atmosphere: dark ambient,^[2,10,102,110,134,162–165,208–211] light ambient,^[51,73,78,89,123,130] nitrogen light/dark,^[41,120,212,213] and dry air dark.^[126]

Moreover, we hope future research focuses on a more profound analysis of the degradation mechanisms in QDSCs. Quite a number of factors (which are listed in **Figure 15**, left hand side) can influence stability of the QDSCs, and by applying a range of structural and spectroscopic characterization methods, it is possible to quantify and evaluate their properties as observables (**Figure 15**, right hand side). Such a detailed investigation—in combination with accurate characterization of the *J*–*V* characteristics evolution—would inevitably enhance the understanding of degradation mechanisms of QD SCs, and expedite the development of mitigation strategies.

6. Conclusions

QD photovoltaics experienced a rapid increase in efficiency with continuous advances in both lead chalcogenide QDSCs and the more recent perovskite QD devices, so that reaching a PCE of 20% is no longer out of sight. Despite this impressive progress, the long-term stability of QDSCs remains a key challenge that

requires significantly more research efforts. In this review, we outlined some of the key developments in understanding mechanisms of degradation of QD materials and photovoltaic devices. While we focused on three different types of QDs, namely, lead chalcogenide, lead halide perovskite, and lead free QDs, all three share plenty commonalities in their fundamental causes for degradation. Ambient factors such as oxygen and water, but also increased temperatures or high intensities of illumination can decrease the lifetime of QDSCs. Beyond these external factors, both the intrinsic properties of QDs and their interplay with other materials present in the photovoltaic devices can also serve as causes of degradation, thus requiring a more detailed analysis. With the focus of the scientific community gradually shifting from enhancing solely the efficiency of the devices to addressing their stability, there is a need for more meticulous approach for the study of fundamental degradation mechanisms in all three types of QDSCs presented here. The elucidation of these degradation mechanisms will allow the development of novel strategies for their mitigation. Unfortunately, the lack of a standardized method to assess stability of

Table 1. Suggested stability measurement conditions for stress-free and realistic tests on QDSCs.

	Stress-free test	Realistic test
Atmosphere	Inert	Air with controlled humidity (e.g., 30% relative humidity)
Temperature	Room temperature (25 °C)	65–85 °C
Illumination	Only for <i>J</i> – <i>V</i> sweep	Continuous illumination (AM1.5)
Bias	Open-circuit	Maximum power point
Encapsulation	Yes	No

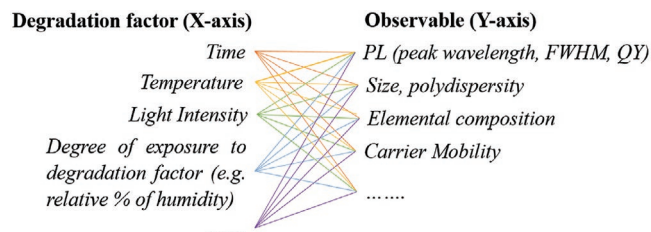


Figure 15. Possible combinations of external factors and material/device characteristics that are helpful in investigations of degradation mechanisms of QDs and QDSCs.

QDSCs limits the applicability of the results across the field. To address this issue, we propose two simple stability tests (stress-free and realistic) which we believe can increase the comparability, reliability, and reproducibility of results and encourage the scientific community to adopt them.

Acknowledgements

The authors acknowledge financial support by the European Research Council (ERC) under the European Union's Horizon 2020 research and innovation program (ERC Grant Agreement No. 714067, ENERGYMAPS). The authors thank the Deutsche Forschungsgemeinschaft (DFG) for funding in the framework of SPP 2196 "Perovskite semiconductors: From fundamental properties to devices" (project (PERFECT PVs), VA 991/3-1 and DE 830/22-1) and the project "PROCES" project (VA 991/2-1). The authors are also grateful for the support by the Croucher Foundation of Hong Kong.

Open access funding enabled and organized by Projekt DEAL.

Conflict of Interest

The authors declare no conflict of interest.

Keywords

degradation, lead chalcogenides, lead halide perovskites, oxidation, passivation, photovoltaics, quantum dots, stability

Received: November 2, 2020

Revised: December 30, 2020

Published online:

- [1] M. Abdelhameed, D. R. Martir, S. Chen, W. Z. Xu, O. O. Oyene, S. Chakrabarti, E. Zysman-Colman, P. A. Charpentier, *Sci. Rep.* **2018**, *8*, 3050.
- [2] C. H. M. Chuang, P. R. Brown, V. Bulović, M. G. Bawendi, *Nat. Mater.* **2014**, *13*, 796.
- [3] X. Dai, Z. Zhang, Y. Jin, Y. Niu, H. Cao, X. Liang, L. Chen, J. Wang, X. Peng, *Nature* **2014**, *515*, 96.
- [4] F. Chen, Q. Lin, H. Shen, A. Tang, *Mater. Chem. Front.* **2020**, *4*, 1340.
- [5] P. J. Pacheco-Linan, I. Bravo, M. L. Nueda, J. Albaladejo, H. Garzón-Ruiz, *ACS Sens.* **2020**, *5*, 2106.
- [6] D. Jung, J. Norman, Y. Wan, S. Liu, R. Herrick, J. Selvidge, K. Mukherjee, A. C. Gossard, J. E. Bowers, *Phys. Status Solidi Appl. Mater. Sci.* **2019**, *216*, 1800602.
- [7] M. Liu, M. Liu, X. Wang, S. M. Kozlov, Z. Cao, P. De Luna, H. Li, X. Qiu, K. Liu, J. Hu, C. Jia, P. Wang, H. Zhou, J. He, M. Zhong, X. Lan, Y. Zhou, Z. Wang, J. Li, A. Seifitokaldani, C. T. Dinh, H. Liang, C. Zou, D. Zhang, Y. Yang, T. S. Chan, Y. Han, L. Cavallo, T. K. Sham, B. J. Hwang, E. H. Sargent, *Joule* **2019**, *3*, 1703.
- [8] H. Borchert, *Solar Cells Based on Colloidal Nanocrystals*, Springer International Publishing, Cham, Switzerland **2014**.
- [9] H. Il Kim, S. W. Baek, H. J. Cheon, S. U. Ryu, S. Lee, M. J. Choi, K. Choi, M. Biondi, S. Hoogland, F. P. G. de Arquer, S. K. Kwon, Y. H. Kim, T. Park, E. H. Sargent, *Adv. Mater.* **2020**, *32*, 2004985.
- [10] M. Hao, Y. Bai, S. Zeiske, L. Ren, J. Liu, Y. Yuan, N. Zarrabi, N. Cheng, M. Ghasemi, P. Chen, M. Lyu, D. He, J. H. Yun, Y. Du, Y. Wang, S. Ding, A. Armin, P. Meredith, G. Liu, H. M. Cheng, L. Wang, *Nat. Energy* **2020**, *5*, 79.
- [11] I. A. Shuklov, V. F. Razumov, *Russ. Chem. Rev.* **2020**, *89*, 379.
- [12] F. W. Wise, *Acc. Chem. Res.* **2000**, *33*, 773.
- [13] D. V. Talapin, C. B. Murray, *Science* **2005**, *310*, 86.
- [14] P. B. Green, P. Narayanan, Z. Li, P. Sohn, C. J. Imperiale, M. W. B. Wilson, *Chem. Mater.* **2020**, *32*, 4083.
- [15] R. Dalven, *Infrared Phys.* **1969**, *9*, 141.
- [16] S. A. McDonald, G. Konstantatos, S. Zhang, P. W. Cyr, E. J. D. Klem, L. Levina, E. H. Sargent, *Nat. Mater.* **2005**, *4*, 138.
- [17] S. W. Baek, S. Jun, B. Kim, A. H. Proppe, O. Ouellette, O. Voznyy, C. Kim, J. Kim, G. Walters, J. H. Song, S. Jeong, H. R. Byun, M. S. Jeong, S. Hoogland, F. P. García de Arquer, S. O. Kelley, J. Y. Lee, E. H. Sargent, *Nat. Energy* **2019**, *4*, 969.
- [18] NREL, NREL PV record efficiency, <https://www.nrel.gov/pv/cell-efficiency.html> (accessed: December 2020).
- [19] C. B. Murray, D. J. Norris, M. G. Bawendi, *J. Am. Chem. Soc.* **1993**, *115*, 8706.
- [20] W. Ma, J. M. Luther, H. Zheng, Y. Wu, A. P. Alivisatos, *Nano Lett.* **2009**, *9*, 1699.
- [21] H. Du, C. Chen, R. Krishnan, T. D. Krauss, J. M. Harbold, F. W. Wise, M. G. Thomas, J. Silcox, *Nano Lett.* **2002**, *2*, 1321.
- [22] M. A. Baghchesara, R. Yousefi, M. Cheraghizade, F. Jamali-Sheini, A. Sa'edi, M. R. Mahmmoudian, *Mater. Res. Bull.* **2016**, *77*, 131.
- [23] H. Goodwin, T. C. Jellicoe, N. J. L. K. Davis, M. L. Böhm, *Nanophotonics* **2018**, *7*, 111.
- [24] M. L. Böhm, T. C. Jellicoe, M. Tabachnyk, N. J. L. K. Davis, F. Wisnivesky-Rocca-Rivarola, C. Ducati, B. Ehrler, A. A. Bakulin, N. C. Greenham, *Nano Lett.* **2015**, *15*, 7987.
- [25] D. Asil, B. J. Walker, B. Ehrler, Y. Vaynzof, A. Sepe, S. Bayliss, A. Sadhanala, P. C. Y. Chow, P. E. Hopkinson, U. Steiner, N. C. Greenham, R. H. Friend, *Adv. Funct. Mater.* **2015**, *25*, 928.
- [26] J. Zhang, J. Gao, C. P. Church, E. M. Miller, J. M. Luther, V. I. Klimov, M. C. Beard, *Nano Lett.* **2014**, *14*, 6010.
- [27] M. H. Zarghami, Y. Liu, M. Gibbs, E. Gebremichael, C. Webster, M. Law, *ACS Nano* **2010**, *4*, 2475.
- [28] B. K. Hughes, D. A. Ruddy, J. L. Blackburn, D. K. Smith, M. R. Bergren, A. J. Nozik, J. C. Johnson, M. C. Beard, *ACS Nano* **2012**, *6*, 5498.
- [29] J. Zhang, J. Gao, E. M. Miller, J. M. Luther, M. C. Beard, *ACS Nano* **2014**, *8*, 614.
- [30] L. Tan, P. Li, B. Sun, M. Chaker, D. Ma, *ACS Energy Lett.* **2017**, *2*, 1573.
- [31] Q. Dai, Y. Wang, Y. Zhang, X. Li, R. Li, B. Zou, J. T. Seo, Y. Wang, M. Liu, W. W. Yu, *Langmuir* **2009**, *25*, 12320.
- [32] M. Sykora, A. Y. Kopysov, J. A. McGuire, R. K. Schulze, O. Tretiak, J. M. Pietryga, V. I. Klimov, *ACS Nano* **2010**, *4*, 2021.
- [33] J. L. Blackburn, H. Chappell, J. M. Luther, A. J. Nozik, J. C. Johnson, *J. Phys. Chem. Lett.* **2011**, *2*, 599.
- [34] G. Konstantatos, L. Levina, A. Fischer, E. H. Sargent, *Nano Lett.* **2008**, *8*, 1446.
- [35] D. Becker-Koch, M. Albaladejo-Siguan, V. Lami, F. Paulus, H. Xiang, Z. Chen, Y. Vaynzof, *Sustainable Energy Fuels* **2020**, *4*, 108.
- [36] N. Zhao, T. P. Osedach, L. Chang, S. M. Geyer, D. Wanger, M. T. Binda, A. C. Arango, M. G. Bawendi, V. Bulovic, *ACS Nano* **2010**, *4*, 3743.
- [37] R. Ihly, J. Tolentino, Y. Liu, M. Gibbs, M. Law, *ACS Nano* **2011**, *5*, 8175.
- [38] K. S. Leschkes, M. S. Kang, E. S. Aydil, D. J. Norris, *J. Phys. Chem. C* **2010**, *114*, 9988.
- [39] J. Z. Fan, N. T. Andersen, M. Biondi, P. Todorović, B. Sun, O. Ouellette, J. Abed, L. K. Sagar, M. J. Choi, S. Hoogland, F. P. G. de Arquer, E. H. Sargent, *Adv. Mater.* **2019**, *31*, 1904304.
- [40] A. R. Kirmani, A. D. Sheikh, M. R. Niazi, M. A. Haque, M. Liu, F. P. G. de Arquer, J. Xu, B. Sun, O. Voznyy, N. Gasparini, D. Baran, T. Wu, E. H. Sargent, A. Amassian, *Adv. Mater.* **2018**, *30*, 1.

- [41] Y. Cao, A. Stavrinadis, T. Lasanta, D. So, G. Konstantatos, *Nat. Energy* **2016**, 1, 16035.
- [42] X. Zhang, D. Jia, C. Häggglund, V. A. Öberg, J. Du, J. Liu, E. M. J. Johansson, *Nano Energy* **2018**, 53, 373.
- [43] H. Choi, J. H. Ko, Y. H. Kim, S. Jeong, *J. Am. Chem. Soc.* **2013**, 135, 5278.
- [44] M. Argeri, A. Fraccarollo, F. Grassi, L. Marchese, M. Cossi, *J. Phys. Chem. C* **2011**, 115, 11382.
- [45] P. Schapotschnikow, M. A. Van Huis, H. W. Zandbergen, D. Vanmaekelbergh, T. J. H. Vlugt, *Nano Lett.* **2010**, 10, 3966.
- [46] L. Lian, Y. Xia, C. Zhang, B. Xu, L. Yang, H. Liu, D. Zhang, K. Wang, J. Gao, J. Zhang, *Chem. Mater.* **2018**, 30, 982.
- [47] L. Tan, Y. Zhou, F. Ren, D. Benetti, F. Yang, H. Zhao, F. Rosei, M. Chaker, D. Ma, *J. Mater. Chem. A* **2017**, 5, 10250.
- [48] D. M. Balazs, K. I. Bijlsma, H. H. Fang, D. N. Dirin, M. Döbeli, M. V. Kovalenko, M. A. Loi, *Sci. Adv.* **2017**, 3, 1558.
- [49] I. Moreels, Y. Justo, B. De Geyter, K. Hastraete, J. C. Martins, Z. Hens, *ACS Nano* **2011**, 5, 2004.
- [50] K. Katsiev, A. H. Ip, A. Fischer, I. Tanabe, X. Zhang, A. R. Kirmani, O. Voznyy, L. R. Rollny, K. W. Chou, S. M. Thon, G. H. Carey, X. Cui, A. Amassian, P. Dowben, E. H. Sargent, O. M. Bakr, *Adv. Mater.* **2014**, 26, 937.
- [51] J. Tang, L. Brzozowski, D. A. R. Barkhouse, X. Wang, R. Debnath, R. Wolowiec, E. Palmiano, L. Levina, A. G. Pattantyus-Abraham, D. Jamakosmanovic, E. H. Sargent, *ACS Nano* **2010**, 4, 869.
- [52] J. Tang, X. Wang, L. Brzozowski, D. A. R. Barkhouse, R. Debnath, L. Levina, E. H. Sargent, *Adv. Mater.* **2010**, 22, 1398.
- [53] J. Y. Woo, J. H. Ko, J. H. Song, K. Kim, H. Choi, Y. H. Kim, D. C. Lee, S. Jeong, *J. Am. Chem. Soc.* **2014**, 136, 8883.
- [54] T. Hacıfendioglu, T. K. Solmaz, M. Erkan, D. Asil, *Sol. Energy Mater. Sol. Cells* **2020**, 207, 110362.
- [55] H. Beygi, S. A. Sajjadi, A. Babakhani, J. F. Young, F. C. J. M. van Veggel, *Appl. Surf. Sci.* **2018**, 457, 1.
- [56] V. Petkov, I. Moreels, Z. Hens, Y. Ren, *Phys. Rev. B: Condens. Matter Phys.* **2010**, 81, 241304.
- [57] Y. Wang, K. Lu, L. Han, Z. Liu, G. Shi, H. Fang, S. Chen, T. Wu, F. Yang, M. Gu, S. Zhou, X. Ling, X. Tang, J. Zheng, M. A. Loi, W. Ma, *Adv. Mater.* **2018**, 30, 1704871.
- [58] M. A. Hines, G. D. Scholes, *Adv. Mater.* **2003**, 15, 1844.
- [59] J. Xu, O. Voznyy, M. M. Liu, A. R. Kirmani, G. Walters, R. Munir, M. Abdelsamie, A. H. Proppe, A. Sarkar, F. P. García De Arquer, M. Wei, B. Sun, M. M. Liu, O. Ouellette, R. Quintero-Bermudez, J. Li, J. Fan, L. Quan, P. Todorovic, H. Tan, S. Hoogland, S. O. Kelley, M. Stefik, A. Amassian, E. H. Sargent, *Nat. Nanotechnol.* **2018**, 13, 456.
- [60] Z. Ren, Z. Kuang, L. Zhang, J. Sun, X. Yi, Z. Pan, X. Zhong, J. Hu, A. Xia, J. Wang, *Sol. RRL* **2017**, 1, 1700176.
- [61] J. Khan, X. Yang, K. Qiao, H. Deng, J. Zhang, Z. Liu, W. Ahmad, J. Zhang, D. Li, H. Liu, H. Song, C. Cheng, J. Tang, *J. Mater. Chem. A* **2017**, 5, 17240.
- [62] T. G. Kim, H. Choi, S. Jeong, J. W. Kim, *J. Phys. Chem. C* **2014**, 118, 27884.
- [63] S. Pradhan, A. Stavrinadis, S. Gupta, G. Konstantatos, *ACS Appl. Mater. Interfaces* **2017**, 9, 27390.
- [64] A. R. Kirmani, F. Eisner, A. E. Mansour, Y. Firdaus, N. Chaturvedi, A. Seitkhan, M. I. Nugraha, E. Yarali, F. P. García de Arquer, E. H. Sargent, T. D. Anthopoulos, A. Amassian, *ACS Appl. Energy Mater.* **2020**, 3, 5135.
- [65] P. R. Brown, R. R. Lunt, N. Zhao, T. P. Osedach, D. D. Wanger, L. Y. Chang, M. G. Bawendi, V. Bulović, *Nano Lett.* **2011**, 11, 2955.
- [66] E. J. D. Klem, H. Shukla, S. Hinds, D. D. MacNeil, L. Levina, E. H. Sargent, *Appl. Phys. Lett.* **2008**, 92, 212105.
- [67] E. J. D. Klem, D. D. MacNeil, L. Levina, E. H. Sargent, *Adv. Mater.* **2008**, 20, 3433.
- [68] J. Xu, O. Voznyy, M. Liu, A. R. Kirmani, G. Walters, R. Munir, M. Abdelsamie, A. H. Proppe, A. Sarkar, F. P. García De Arquer, M. Wei, B. Sun, M. Liu, O. Ouellette, R. Quintero-Bermudez, J. Li, J. Fan, L. Quan, P. Todorovic, H. Tan, S. Hoogland, S. O. Kelley, M. Stefik, A. Amassian, E. H. Sargent, *Nat. Nanotechnol.* **2018**, 13, 456.
- [69] Q. Lin, H. J. Yun, W. Liu, H. J. Song, N. S. Makarov, O. Isaienko, T. Nakotte, G. Chen, H. Luo, V. I. Klimov, J. M. Pietryga, *J. Am. Chem. Soc.* **2017**, 139, 6644.
- [70] D. Jia, J. Chen, S. Zheng, D. Phuyal, M. Yu, L. Tian, J. Liu, O. Karis, H. Rensmo, E. M. J. Johansson, X. Zhang, *Adv. Energy Mater.* **2019**, 9, 1.
- [71] M. Albaladejo-Siguan, D. Becker-Koch, A. D. Taylor, Q. Sun, V. Lami, P. G. Oppenheimer, F. Paulus, Y. Vaynzof, *ACS Nano* **2020**, 14, 384.
- [72] P. R. Brown, D. Kim, R. R. Lunt, N. Zhao, M. G. Bawendi, J. C. Grossman, V. Bulović, *ACS Nano* **2014**, 8, 5863.
- [73] R. Azmi, S. Y. Nam, S. Sinaga, S. H. Oh, T. K. Ahn, S. C. Yoon, I. H. Jung, S. Y. Jang, *Nano Energy* **2017**, 39, 355.
- [74] J. M. Salazar-Rios, N. Sukharevska, M. J. Speirs, S. Jung, D. Dirin, R. M. Dragoman, S. Allard, M. V. Kovalenko, U. Scherf, M. A. Loi, *Adv. Mater. Interfaces* **2018**, 5, 1801155.
- [75] B. Martín-García, Y. Bi, M. Prato, D. Spirito, R. Krahne, G. Konstantatos, I. Moreels, *Sol. Energy Mater. Sol. Cells* **2018**, 183, 1.
- [76] J. Z. Fan, A. D. La Croix, Z. Yang, E. Howard, R. Quintero-Bermudez, L. Levina, N. M. Jenkinson, N. J. Spear, Y. Li, O. Ouellette, Z. H. Lu, E. H. Sargent, J. E. Macdonald, *Nanoscale* **2019**, 11, 10774.
- [77] S. Liu, L. Hu, S. Huang, W. Zhang, J. Ma, J.-C. Wang, X. Guan, C.-H. Lin, J. Kim, T. WAN, Q. Lei, D. Chu, T. Wu, *ACS Appl. Mater. Interfaces* **2020**, 12, 46239.
- [78] B. Sun, A. Johnston, C. Xu, M. Wei, Z. Huang, Z. Jiang, H. Zhou, Y. Gao, Y. Dong, O. Ouellette, X. Zheng, J. Liu, M. J. Choi, Y. Gao, S. W. Baek, F. Laquai, O. M. Bakr, D. Ban, O. Voznyy, F. P. García de Arquer, E. H. Sargent, *Joule* **2020**, 4, 1542.
- [79] M. Biondi, M. J. Choi, O. Ouellette, S. W. Baek, P. Todorović, B. Sun, S. Lee, M. Wei, P. Li, A. R. Kirmani, L. K. Sagar, L. J. Richter, S. Hoogland, Z. H. Lu, F. P. García de Arquer, E. H. Sargent, *Adv. Mater.* **2020**, 32, 1906199.
- [80] H. Aqoma, M. Al Mubarak, W. Lee, W. T. Hadmojo, C. Park, T. K. Ahn, D. Y. Ryu, S. Y. Jang, *Adv. Energy Mater.* **2018**, 8, 1800572.
- [81] M. Al Mubarak, F. Tri, A. Wibowo, H. Aqoma, N. V. Krishna, W. Lee, D. Y. Ryu, S. Cho, I. H. Jung, S. Jang, *Adv. Energy Mater.* **2020**, 10, 1902933.
- [82] H. Lim, D. Kim, M. J. Choi, E. H. Sargent, Y. S. Jung, J. Y. Kim, *Adv. Energy Mater.* **2019**, 9, 1901938.
- [83] H. Tavakoli Dastjerdi, P. Qi, Z. Fan, M. M. Tavakoli, *ACS Appl. Mater. Interfaces* **2020**, 12, 818.
- [84] Y. Xue, F. Yang, J. Yuan, Y. Zhang, M. Gu, Y. Xu, X. Ling, Y. Wang, F. Li, T. Zhai, J. Li, C. Cui, Y. Chen, W. Ma, *ACS Energy Lett.* **2019**, 4, 2850.
- [85] G. Yang, Y. Zhu, J. Huang, X. Xu, S. Cui, Z. Lu, *Opt. Express* **2019**, 27, A1338.
- [86] B. Kan, M. Li, Q. Zhang, F. Liu, X. Wan, Y. Wang, W. Ni, G. Long, X. Yang, H. Feng, Y. Zuo, M. Zhang, F. Huang, Y. Cao, T. P. Russell, Y. Chen, *J. Am. Chem. Soc.* **2015**, 137, 3886.
- [87] Y. J. Jeong, J. H. Song, S. Jeong, S. J. Baik, *IEEE J. Photovoltaics* **2018**, 8, 493.
- [88] D. C. J. Neo, N. Zhang, Y. Tazawa, H. Jiang, G. M. Hughes, C. R. M. Grovenor, H. E. Assender, A. A. R. Watt, *ACS Appl. Mater. Interfaces* **2016**, 8, 12101.
- [89] J. Choi, M. J. Choi, J. Kim, F. Dinic, P. Todorovic, B. Sun, M. Wei, S. W. Baek, S. Hoogland, F. P. García de Arquer, O. Voznyy, E. H. Sargent, *Adv. Mater.* **2020**, 32, 1906497.

- [90] Z. Zhang, Z. Chen, J. Zhang, W. Chen, J. Yang, X. Wen, B. Wang, N. Kobamoto, L. Yuan, J. A. Stride, G. J. Conibeer, R. J. Patterson, S. Huang, *Adv. Energy Mater.* **2017**, 7, 1601773.
- [91] Z. Zhang, Z. Chen, L. Yuan, W. Chen, J. Yang, B. Wang, X. Wen, J. Zhang, L. Hu, J. A. Stride, G. J. Conibeer, R. J. Patterson, S. Huang, *Adv. Mater.* **2017**, 29, 1703214.
- [92] L. Hu, X. Geng, S. Singh, J. Shi, Y. Hu, S. Li, X. Guan, T. He, X. Li, Z. Cheng, R. Patterson, S. Huang, T. Wu, *Nano Energy* **2019**, 64, 103922.
- [93] S. Kim, A. R. Marshall, D. M. Kroupa, E. M. Miller, J. M. Luther, S. Jeong, M. C. Beard, *ACS Nano* **2015**, 9, 8157.
- [94] A. R. Marshall, M. R. Young, A. J. Nozik, M. C. Beard, J. M. Luther, *J. Phys. Chem. Lett.* **2015**, 6, 2892.
- [95] W. K. Bae, J. Joo, L. A. Padilha, J. Won, D. C. Lee, Q. Lin, W. K. Koh, H. Luo, V. I. Klimov, J. M. Pietryga, *J. Am. Chem. Soc.* **2012**, 134, 20160.
- [96] Z. Zhang, J. Yang, X. Wen, L. Yuan, S. Shrestha, J. A. Stride, G. J. Conibeer, R. J. Patterson, S. Huang, *J. Phys. Chem. C* **2015**, 119, 24149.
- [97] Y. Zhang, C. Ding, G. Wu, N. Nakazawa, J. Chang, Y. Ogomi, T. Toyoda, S. Hayase, K. Katayama, Q. Shen, *J. Phys. Chem. C* **2016**, 120, 28509.
- [98] R. W. Crisp, D. M. Kroupa, A. R. Marshall, E. M. Miller, J. Zhang, M. C. Beard, J. M. Luther, *Sci. Rep.* **2015**, 5, 9945.
- [99] X. Lan, O. Voznyy, A. Kiani, F. P. García De Arquer, A. S. Abbas, G. H. Kim, M. Liu, Z. Yang, G. Walters, J. Xu, M. Yuan, Z. Ning, F. Fan, P. Kanjanaboos, I. Kramer, D. Zhitomirsky, P. Lee, A. Perelgut, S. Hoogland, E. H. Sargent, *Adv. Mater.* **2016**, 28, 299.
- [100] J. Y. Woo, S. Lee, S. Lee, W. D. Kim, K. Lee, K. Kim, H. J. An, D. C. Lee, S. Jeong, *J. Am. Chem. Soc.* **2016**, 138, 876.
- [101] L. Hu, Z. Zhang, R. J. Patterson, S. B. Shivarudraiah, Z. Zhou, M. Ng, S. Huang, J. E. Halpert, *Sol. RRL* **2018**, 2, 1800234.
- [102] J. Tang, K. W. Kemp, S. Hoogland, K. S. Jeong, H. Liu, L. Levina, M. Furukawa, X. Wang, R. Debnath, D. Cha, K. W. Chou, A. Fischer, A. Amassian, J. B. Asbury, E. H. Sargent, *Nat. Mater.* **2011**, 10, 765.
- [103] W. Ahmad, J. He, Z. Liu, K. Xu, Z. Chen, X. Yang, D. Li, Y. Xia, J. Zhang, C. Chen, *Adv. Mater.* **2019**, 31, 1.
- [104] W. D. Lawson, *J. Appl. Phys.* **1952**, 23, 495.
- [105] G. Liu, C. Yan, Z. J. Xue, C. Liu, G. Xu, T. Wang, *Nanoscale* **2018**, 10, 12284.
- [106] A. H. Ip, A. J. Labelle, E. H. Sargent, *Appl. Phys. Lett.* **2013**, 103, 263905.
- [107] Y. Li, X. Zhang, H. Huang, S. V. Kershaw, A. L. Rogach, *Mater. Today* **2020**, 32, 204.
- [108] H. Huang, M. I. Bodnarchuk, S. V. Kershaw, M. V. Kovalenko, A. L. Rogach, *ACS Energy Lett.* **2017**, 2, 2071.
- [109] A. O. El-Ballouli, O. M. Bakr, O. F. Mohammed, *Chem. Mater.* **2019**, 31, 6387.
- [110] J. Xue, J. W. Lee, Z. Dai, R. Wang, S. Nuryyeva, M. E. Liao, S. Y. Chang, L. Meng, D. Meng, P. Sun, O. Lin, M. S. Goorsky, Y. Yang, *Joule* **2018**, 2, 1866.
- [111] Q. Tai, K.-C. Tang, F. Yan, *Energy Environ. Sci.* **2019**, 12, 2375.
- [112] F. Bella, P. Renzi, C. Cavallo, C. Gerbaldi, *Chemistry* **2018**, 24, 12183.
- [113] A. Kojima, K. Teshima, Y. Shirai, T. Miyasaka, *J. Am. Chem. Soc.* **2009**, 131, 6050.
- [114] F. Zu, T. Schultz, D. Shin, L. Frohloff, P. Amsalem, N. Koch, C. M. Wolff, D. Neher, T. Schultz, N. Koch, *RSC Adv.* **2020**, 10, 17534.
- [115] C. Li, A. Guerrero, S. Huettner, J. Bisquert, *Nat. Commun.* **2018**, 9, 5113.
- [116] R. J. Sutton, M. R. Filip, A. A. Haghighirad, N. Sakai, B. Wenger, F. Giustino, H. J. Snaith, *ACS Energy Lett.* **2018**, 3, 1787.
- [117] A. Marronnier, G. Roma, S. Boyer-Richard, L. Pedesseau, J.-M. Jancu, Y. Bonnassieux, C. Katan, C. C. Stoumpos, M. G. Kanatzidis, J. Even, *ACS Nano* **2018**, 12, 3477.
- [118] C. C. Stoumpos, M. G. Kanatzidis, *Acc. Chem. Res.* **2015**, 48, 2791.
- [119] Q. Zhao, A. Hazarika, L. T. Schelhas, J. Liu, E. A. Gaulding, G. Li, M. Zhang, M. F. Toney, P. C. Sercel, J. M. Luther, *ACS Energy Lett.* **2020**, 5, 238.
- [120] A. Swarnkar, A. R. Marshall, E. M. Sanehira, B. D. Chernomordik, D. T. Moore, J. A. Christians, T. Chakrabarti, J. M. Luther, *Science* **2016**, 354, 92.
- [121] L. Protesescu, S. Yakunin, M. I. Bodnarchuk, F. Krieg, R. Caputo, C. H. Hendon, R. X. Yang, A. Walsh, M. V. Kovalenko, *Nano Lett.* **2015**, 15, 3692.
- [122] J. Yuan, C. Bi, S. Wang, R. Guo, T. Shen, L. Zhang, J. Tian, *Adv. Funct. Mater.* **2019**, 29, 1906615.
- [123] Q. Zhao, A. Hazarika, X. Chen, S. P. Harvey, B. W. Larson, G. R. Teeter, J. Liu, T. Song, C. Xiao, L. Shaw, M. Zhang, G. Li, M. C. Beard, J. M. Luther, *Nat. Commun.* **2019**, 10, 2842.
- [124] L. M. Wheeler, E. M. Sanehira, A. R. Marshall, P. Schulz, M. Suri, N. C. Anderson, J. A. Christians, D. Nordlund, D. Sokaras, T. Kroll, S. P. Harvey, J. J. Berry, L. Y. Lin, J. M. Luther, *J. Am. Chem. Soc.* **2018**, 140, 10504.
- [125] V. M. Goldschmidt, *Naturwissenschaften* **1926**, 14, 477.
- [126] Q. Zeng, X. Zhang, X. Feng, S. Lu, Z. Chen, X. Yong, S. A. T. Redfern, H. Wei, H. Wang, H. Shen, W. Zhang, W. Zheng, H. Zhang, J. S. Tse, B. Yang, *Adv. Mater.* **2018**, 30, 1705393.
- [127] S. Christodoulou, F. Di Stasio, S. Pradhan, A. Stavrinadis, G. Konstantatos, *J. Phys. Chem. C* **2018**, 122, 7621.
- [128] D. Ghosh, M. Y. Ali, D. K. Chaudhary, S. Bhattacharyya, *Sol. Energy Mater. Sol. Cells* **2018**, 185, 28.
- [129] Y. Lin, B. Chen, F. Zhao, X. Zheng, Y. Deng, Y. Shao, Y. Fang, Y. Bai, C. Wang, J. Huang, *Adv. Mater.* **2017**, 29, 1700607.
- [130] D. B. Khadka, Y. Shirai, M. Yanagida, T. Noda, K. Miyano, *ACS Appl. Mater. Interfaces* **2018**, 10, 22074.
- [131] A. Hazarika, Q. Zhao, E. A. Gaulding, J. A. Christians, B. Dou, A. R. Marshall, T. Moot, J. J. Berry, J. C. Johnson, J. M. Luther, *ACS Nano* **2018**, 12, 10327.
- [132] C. F. J. Lau, M. Zhang, X. Deng, J. Zheng, J. Bing, Q. Ma, J. Kim, L. Hu, M. A. Green, S. Huang, A. Ho-Baillie, *ACS Energy Lett.* **2017**, 2, 2319.
- [133] W. van der Stam, J. J. Geuchies, T. Altantzis, K. H. W. van den Bos, J. D. Meeldijk, S. Van Aert, S. Bals, D. Vanmaekelbergh, C. de Mello Donega, *J. Am. Chem. Soc.* **2017**, 139, 4087.
- [134] J. Shi, F. Li, J. Yuan, X. Ling, S. Zhou, Y. Qian, W. Ma, *J. Mater. Chem. A* **2019**, 7, 20936.
- [135] W. Liu, Q. Lin, H. Li, K. Wu, I. Robel, J. M. Pietryga, V. I. Klimov, *J. Am. Chem. Soc.* **2016**, 138, 14954.
- [136] J. Zhu, X. Yang, Y. Zhu, Y. Wang, J. Cai, J. Shen, L. Sun, C. Li, *J. Phys. Chem. Lett.* **2017**, 8, 4167.
- [137] Q. Wang, X. Zhang, Z. Jin, J. Zhang, Z. Gao, Y. Li, S. F. Liu, *ACS Energy Lett.* **2017**, 2, 1479.
- [138] F. Liu, C. Ding, Y. Zhang, T. Kamisaka, Q. Zhao, J. M. Luther, T. Toyoda, S. Hayase, T. Minemoto, K. Yoshino, B. Zhang, S. Dai, J. Jiang, S. Tao, Q. Shen, *Chem. Mater.* **2019**, 31, 798.
- [139] W. Gao, C. Ran, J. Xi, B. Jiao, W. Zhang, M. Wu, X. Hou, Z. Wu, *ChemPhysChem* **2018**, 19, 1696.
- [140] M. Lu, X. Zhang, X. Bai, H. Wu, X. Shen, Y. Zhang, W. Zhang, W. Zheng, H. Song, W. Yu, A. L. Rogach, *ACS Energy Lett.* **2018**, 3, 1571.
- [141] F. Hao, C. C. Stoumpos, R. P. H. Chang, M. G. Kanatzidis, *J. Am. Chem. Soc.* **2014**, 136, 8094.
- [142] J.-S. Yao, J. Ge, B.-N. Han, K.-H. Wang, H.-B. Yao, H.-L. Yu, J.-H. Li, B.-S. Zhu, J.-Z. Song, C. Chen, Q. Zhang, H.-B. Zeng, Y. Luo, S.-H. Yu, *J. Am. Chem. Soc.* **2018**, 140, 3626.
- [143] A. D. Jodlowski, C. Roldán-Carmona, G. Grancini, M. Salado, M. Ralaifarisoa, S. Ahmad, N. Koch, L. Camacho, G. De Miguel, M. K. Nazeeruddin, *Nat. Energy* **2017**, 2, 972.

- [144] X. Ling, J. Yuan, X. Zhang, Y. Qian, S. M. Zakeeruddin, B. W. Larson, Q. Zhao, J. Shi, J. Yang, K. Ji, Y. Zhang, Y. Wang, C. Zhang, S. Duhm, J. M. Luther, M. Grätzel, W. Ma, *Adv. Mater.* **2020**, *32*, 2001906.
- [145] D. V. Talapin, R. Koeppel, S. Götzinger, A. Kornowski, J. M. Lupton, A. L. Rogach, O. Benson, J. Feldmann, H. Weller, *Nano Lett.* **2003**, *3*, 1677.
- [146] O. Chen, J. Zhao, V. P. Chauhan, J. Cui, C. Wong, D. K. Harris, H. Wei, H. S. Han, D. Fukumura, R. K. Jain, M. G. Bawendi, *Nat. Mater.* **2013**, *12*, 445.
- [147] X. Zhang, W. Yin, W. Zheng, A. L. Rogach, *ACS Energy Lett.* **2020**, *5*, 2927.
- [148] Z. Ning, X. Gong, R. Comin, G. Walters, F. Fan, O. Voznyy, E. Yassitepe, A. Buin, S. Hoogland, E. H. Sargent, *Nature* **2015**, *523*, 324.
- [149] M. Sytnyk, S. Yakunin, W. Schöfberger, R. T. Lechner, M. Burian, L. Ludescher, N. A. Killilea, A. Yousefamin, D. Kriegner, J. Stangl, H. Groiss, W. Heiss, *ACS Nano* **2017**, *11*, 1246.
- [150] S. Wang, C. Bi, A. Portniagin, J. Yuan, J. Ning, X. Xiao, X. Zhang, Y. Y. Li, S. V. Kershaw, J. Tian, A. L. Rogach, *ACS Energy Lett.* **2020**, *5*, 2401.
- [151] V. K. Ravi, S. Saikia, S. Yadav, V. V. Nawale, A. Nag, *ACS Energy Lett.* **2020**, *5*, 1794.
- [152] Q. Wen, S. V. Kershaw, S. Kalytchuk, O. Zhovtiuk, C. Reckmeier, M. I. Vasilevskiy, A. L. Rogach, *ACS Nano* **2016**, *10*, 4301.
- [153] Y. Li, H. Huang, Y. Xiong, S. V. Kershaw, A. L. Rogach, *CrystEngComm* **2018**, *20*, 4900.
- [154] K. Chen, Q. Zhong, W. Chen, B. Sang, Y. Wang, T. Yang, Y. Liu, Y. Zhang, H. Zhang, *Adv. Funct. Mater.* **2019**, *29*, 1900991.
- [155] I. C. Smith, E. T. Hoke, D. Solis-Ibarra, M. D. McGehee, H. I. Karunadasa, *Angew. Chem., Int. Ed. Engl.* **2014**, *53*, 11232.
- [156] C. C. Stoumpos, D. H. Cao, D. J. Clark, J. Young, J. M. Rondinelli, J. I. Jang, J. T. Hupp, M. G. Kanatzidis, *Chem. Mater.* **2016**, *28*, 2852.
- [157] L. N. Quan, M. Yuan, R. Comin, O. Voznyy, E. M. Beauregard, S. Hoogland, A. Buin, A. R. Kirmani, K. Zhao, A. Amassian, D. H. Kim, E. H. Sargent, *J. Am. Chem. Soc.* **2016**, *138*, 2649.
- [158] L. Na Quan, D. Ma, Y. Zhao, O. Voznyy, H. Yuan, E. Bladt, J. Pan, F. P. García de Arquer, R. Sabatini, Z. Piontkowski, A. H. Emwas, P. Todorović, R. Quintero-Bermudez, G. Walters, J. Z. Fan, M. Liu, H. Tan, M. I. Saidaminov, L. Gao, Y. Li, D. H. Anjum, N. Wei, J. Tang, D. W. McCamant, M. B. J. Roeffaers, S. Bals, J. Hofkens, O. M. Bakr, Z. H. Lu, E. H. Sargent, *Nat. Commun.* **2020**, *11*, 170.
- [159] J. Zhang, D. Bai, Z. Jin, H. Bian, K. Wang, J. Sun, Q. Wang, S. F. Liu, *Adv. Energy Mater.* **2018**, *8*, 1703246.
- [160] E. M. Sanehira, A. R. Marshall, J. A. Christians, S. P. Harvey, P. N. Ciesielski, L. M. Wheeler, P. Schulz, L. Y. Lin, M. C. Beard, J. M. Luther, *Sci. Adv.* **2017**, *3*, 4204.
- [161] K. Usman, S. Ming, X. Liu, X. Li, Z. Gui, Q. Xie, W. Zhang, Y. Wu, H. Q. Wang, J. Fang, *Appl. Nanosci.* **2018**, *8*, 715.
- [162] F. Li, S. Zhou, J. Yuan, C. Qin, Y. Yang, J. Shi, X. Ling, Y. Li, W. Ma, *ACS Energy Lett.* **2019**, *4*, 2571.
- [163] Q. Wang, Z. Jin, D. Chen, D. Bai, H. Bian, J. Sun, G. Zhu, G. Wang, S. (Frank) Liu, *Adv. Energy Mater.* **2018**, *8*, 1800007.
- [164] J. Yuan, X. Ling, D. Yang, F. Li, S. Zhou, J. Shi, Y. Qian, J. Hu, Y. Sun, Y. Yang, X. Gao, S. Duhm, Q. Zhang, W. Ma, *Joule* **2018**, *2*, 2450.
- [165] X. Ling, S. Zhou, J. Yuan, J. Shi, Y. Qian, B. W. Larson, Q. Zhao, C. Qin, F. Li, G. Shi, C. Stewart, J. Hu, X. Zhang, J. M. Luther, S. Duhm, W. Ma, *Adv. Energy Mater.* **2019**, *9*, 1900721.
- [166] G. H. Carey, A. L. Abdelhady, Z. Ning, S. M. Thon, O. M. Bakr, E. H. Sargent, *Chem. Rev.* **2015**, *115*, 12732.
- [167] D. Eun, L. Soo, Y. Kim, H. Won, *J. Korean Ceram. Soc.* **2020**, *57*, 455.
- [168] P. K. Santra, P. V. Kamat, *J. Am. Chem. Soc.* **2012**, *134*, 2508.
- [169] S. Yang, P. Zhao, X. Zhao, L. Qu, X. Lai, J. Mater. Chem. A **2015**, *3*, 21922.
- [170] V. A. Öberg, M. B. Johansson, X. Zhang, E. M. J. Johansson, *ACS Appl. Nano Mater.* **2020**, *7*, 1020.
- [171] J. D. Major, R. E. Treharne, L. J. Phillips, K. Durose, *Nature* **2014**, *511*, 334.
- [172] S. Sadeghi, S. K. Abkenar, C. W. Ow-yang, S. Nizamoglu, *Sci. Rep.* **2019**, *9*, 1.
- [173] Z. Pan, K. Zhao, J. Wang, H. Zhang, Y. Feng, X. Zhong, *ACS Nano* **2013**, *7*, 5215.
- [174] M. Bernechea, N. C. Miller, G. Xercavins, D. So, A. Stavrinadis, G. Konstantatos, *Nat. Photonics* **2016**, *10*, 521.
- [175] K. Boldt, O. T. Bruns, N. Gaponik, A. Eychmüller, *J. Phys. Chem. B* **2006**, *110*, 1959.
- [176] K. Susumu, H. T. Uyeda, I. L. Medintz, T. Pons, J. B. Delehanty, H. Mattoussi, *J. Am. Chem. Soc.* **2007**, *129*, 13987.
- [177] Y. Zhang, Y. Chen, P. Westerhoff, J. C. Crittenden, *Environ. Sci. Technol.* **2008**, *42*, 321.
- [178] K. Schilling, H. Weller, A. Eychmüller, *Phys. Chem. Chem. Phys.* **2002**, *4*, 4747.
- [179] J. Aldana, Y. A. Wang, X. Peng, *J. Am. Chem. Soc.* **2001**, *123*, 8844.
- [180] T. Pons, H. T. Uyeda, I. L. Medintz, H. Mattoussi, *J. Phys. Chem. B* **2006**, *110*, 20308.
- [181] W. R. Algar, U. J. Krull, *Chem. Phys. Chem* **2007**, *8*, 561.
- [182] Z. J. Zhu, Y. C. Yeh, R. Tang, B. Yan, J. Tamayo, R. W. Vachet, V. M. Rotello, *Nat. Chem.* **2011**, *3*, 963.
- [183] W. J. Jin, J. M. Costa-Fernández, R. Pereiro, A. Sanz-Medel, *Anal. Chim. Acta* **2004**, *522*, 1.
- [184] W. G. J. H. M. Van Sark, P. L. T. M. Frederix, D. J. Van Den Heuvel, A. A. Bol, J. N. J. Van Ling, C. De Mello Donegá, H. C. Gerritsen, A. Meijerink, *J. Fluoresc.* **2002**, *12*, 69.
- [185] J. E. Bowen Katari, V. L. Colvin, A. P. Alivisatos, *J. Phys. Chem.* **1994**, *98*, 15.
- [186] C. Zhang, S. O'Brien, L. Balogh, *J. Phys. Chem. B* **2002**, *106*, 10316.
- [187] R. Calzada, C. M. Thompson, D. E. Westmoreland, K. Edme, E. A. Weiss, *Chem. Mater.* **2016**, *28*, 6716.
- [188] M. Yu, G. W. Fernando, R. Li, F. Papadimitrakopoulos, N. Shi, R. Ramprasad, *Appl. Phys. Lett.* **2006**, *88*, 15.
- [189] M. Grabolle, J. Ziegler, A. Merkulov, T. Nann, U. Resch-Genger, *Ann. N. Y. Acad. Sci.* **2008**, *1130*, 235.
- [190] X. Wang, L. Qu, J. Zhang, X. Peng, M. Xiao, *Nano Lett.* **2003**, *3*, 1103.
- [191] C. F. Landes, M. Braun, M. A. El-Sayed, *J. Phys. Chem. B* **2001**, *105*, 10554.
- [192] M. Jiong, J. Y. Cnen, Y. Zhang, P. N. Wang, J. Guo, W. L. Yang, C. C. Wang, *J. Phys. Chem. B* **2007**, *111*, 12012.
- [193] J. Lim, W. K. Bae, D. Lee, M. K. Nam, J. Jung, C. Lee, K. Char, S. Lee, *Chem. Mater.* **2011**, *23*, 4459.
- [194] Y. Zhao, C. Riemersma, F. Pietra, R. Koole, C. De Mello Donegá, A. Meijerink, *ACS Nano* **2012**, *6*, 9058.
- [195] B. Xing, W. Li, H. Dou, P. Zhang, K. Sun, *J. Phys. Chem. C* **2008**, *112*, 14318.
- [196] X. Yuan, J. Zheng, R. Zeng, P. Jing, W. Ji, J. Zhao, W. Yang, H. Li, *Nanoscale* **2014**, *6*, 300.
- [197] C. Kagan, C. B. Murray, M. G. Bawendi, *Phys. Rev. B* **1996**, *54*, 8633.
- [198] Y. Tan, S. Jin, R. J. Hamers, *ACS Appl. Mater. Interfaces* **2013**, *5*, 12975.
- [199] S. R. Cordero, P. J. Carson, R. A. Estabrook, G. F. Strouse, S. K. Buratto, *J. Phys. Chem. B* **2000**, *104*, 12137.
- [200] K. Zhang, W. He, L. Wu, G. Xu, S. Ji, C. Ye, *RSC Adv.* **2014**, *4*, 15702.
- [201] C. Liu, L. Mu, J. Jia, X. Zhou, Y. Lin, *Electrochim. Acta* **2013**, *111*, 179.
- [202] J. Luo, H. Wei, Q. Huang, X. Hu, H. Zhao, R. Yu, D. Li, Y. Luo, Q. Meng, *Chem. Commun.* **2013**, *49*, 3881.

- [203] M. G. Panthani, J. M. Kurley, R. W. Crisp, T. C. Dietz, T. Ezzyat, J. M. Luther, D. V. Talapin, *Nano Lett.* **2014**, *14*, 670.
- [204] I. Gur, N. a Fromer, M. L. Geier, A. P. Alivisatos, *Science* **2005**, *310*, 462.
- [205] K. Tvrđy, P. V. Kamat, *J. Phys. Chem. A* **2009**, *113*, 3765.
- [206] D. A. Hines, M. A. Becker, P. V. Kamat, *J. Phys. Chem. C* **2012**, *116*, 13452.
- [207] K. Ji, J. Yuan, F. Li, Y. Shi, X. Ling, X. Zhang, Y. Zhang, H. Lu, J. Yuan, W. Ma, *J. Mater. Chem. A* **2020**, *8*, 8104.
- [208] B. Hou, Y. Cho, B. S. Kim, J. Hong, J. B. Park, S. J. Ahn, J. I. Sohn, S. Cha, J. M. Kim, *ACS Energy Lett.* **2016**, *1*, 834.
- [209] S. Pradhan, A. Stavrinadis, S. Gupta, S. Christodoulou, G. Konstantatos, *ACS Energy Lett.* **2017**, *2*, 1444.
- [210] A. R. Kirmani, F. P. García De Arquer, J. Z. Fan, J. I. Khan, G. Walters, S. Hoogland, N. Wehbe, M. M. Said, S. Barlow, F. Laquai, S. R. Marder, E. H. Sargent, A. Amassian, *ACS Energy Lett.* **2017**, *2*, 1952.
- [211] M. Liu, O. Voznyy, R. Sabatini, F. P. García de Arquer, R. Munir, A. H. Balawi, X. Lan, F. Fan, G. Walters, A. R. Kirmani, S. Hoogland, F. Laquai, A. Amassian, E. H. Sargent, *Nat. Mater.* **2017**, *16*, 258.
- [212] A. H. Ip, S. M. Thon, S. Hoogland, O. Voznyy, D. Zhitomirsky, R. Debnath, L. Levina, L. R. Rollny, G. H. Carey, A. Fischer, K. W. Kemp, I. J. Kramer, Z. Ning, A. J. Labelle, K. W. Chou, A. Amassian, E. H. Sargent, *Nat. Nanotechnol.* **2012**, *7*, 577.
- [213] L.-H. Lai, M. J. Speirs, F.-K. Chang, L. Piveteau, M. V. Kovalenko, J.-S. Chen, J.-J. Wu, M. A. Loi, *Appl. Phys. Lett.* **2015**, *107*, 183901.
- [214] P. Holzhey, M. Saliba, *J. Mater. Chem. A* **2018**, *6*, 21794.
- [215] M. V. Khenkin, E. A. Katz, A. Abate, G. Bardizza, J. J. Berry, C. Brabec, F. Brunetti, V. Bulović, Q. Burlingame, A. Di Carlo, R. Cheacharoen, Y. B. Cheng, A. Colsmann, S. Cros, K. Domanski, M. Duszka, C. J. Fell, S. R. Forrest, Y. Galagan, D. Di Girolamo, M. Grätzel, A. Hagfeldt, E. von Hauff, H. Hoppe, J. Kettle, H. Köbler, M. S. Leite, S. (Frank) Liu, Y. L. Loo, J. M. Luther, C. Q. Ma, M. Madsen, M. Manceau, M. Matheron, M. McGehee, R. Meitzner, M. K. Nazeeruddin, A. F. Nogueira, Ç. Odabaşı, A. Osherov, N. G. Park, M. O. Reese, F. De Rossi, M. Saliba, U. S. Schubert, H. J. Snaith, S. D. Stranks, W. Tress, P. A. Troshin, V. Turkovic, S. Veenstra, I. Visoly-Fisher, A. Walsh, T. Watson, H. Xie, R. Yıldırım, S. M. Zakeeruddin, K. Zhu, M. Lira-Cantu, *Nat. Energy* **2020**, *5*, 35.



Miguel Albaladejo-Siguan is a doctoral student at the Integrated Centre for Applied Physics and Photonic Materials at the Technical University of Dresden. He obtained his bachelor and master's degrees from Heidelberg University. His research interests include the synthesis and characterization of core-shell quantum dot heterostructures and the development of passivation strategies for improving the stability of quantum dot solar cells.



Yanxiu Li is a postdoctoral research fellow at the Integrated Centre for Applied Physics and Photonic Materials at the Technical University of Dresden. She obtained her Ph.D. at the City University of Hong Kong, under the supervision of Prof. Andrey L. Rogach where she developed synthetic routes for dimension and geometry control of perovskite quantum dots. Her current research involves the integration of perovskite quantum dots into photovoltaic devices, focusing on optimizing the device performance and stability.



Yana Vaynzof is the Chair for Emerging Electronic Technologies at the Integrated Centre for Applied Physics and Photonic Materials at the Technical University of Dresden. She obtained her Ph.D. in Physics from the University of Cambridge and a Master in Electrical Engineering from Princeton University. Her research interests focus on emerging photovoltaics based on organic, perovskite and colloidal quantum dot materials and the development of spectroscopic methods for the study of their material physics.